UNIVERSITY OF CAMBRIDGE | Energy Policy Research Group

Simulation and Evaluation of Zonal Electricity Market Designs

EPRG Working Paper 1813

Cambridge Working Paper in Economics 1829

M. R. Hesamzadeh, P. Holmberg, M. Sarfati

Abstract Zonal pricing with countertrading (a market-based redispatch) gives arbitrage opportunities to the power producers located in the export-constrained nodes. They can increase their profit by increasing the output in the day-ahead market and decrease it in the real-time market (the inc-dec game). We show that this leads to large inefficiencies in a standard zonal market. We also show how the inefficiencies can be significantly mitigated by changing the design of the real-time market. We consider a two-stage game with oligopoly producers, wind-power shocks and real-time shocks. The game is formulated as a two-stage stochastic equilibrium problem with equilibrium constraints (EPEC), which we recast into a two-stage stochastic Mixed-Integer Bilinear Program (MIBLP). We present numerical results for a six-node and the IEEE 24-node system.

Keywords Two-stage game, Zonal pricing, Wholesale electricity market, Bilinear programming

JEL Classification C61, C63, C72, D43, D47, L13, L94

Contact par.holmberg@ifn.se
Publication May 2018
Financial Support SweGRIDS, Swedish Energy Agency, Torsten Söderberg Foundation, Jan Wallander and Tom Hedelius Foundation

Simulation and Evaluation of Zonal Electricity Market Designs[☆]
May 2, 2018

M. R. Hesamzadeh[a], P. Holmberg[b,c], M. Sarfati[b]

[a] *Electricity Market Research Group (EMReG), KTH Royal Institute of Technology, Sweden*
[b] *Research Institute of Industrial Economics (IFN), Sweden*
[c] *Energy Policy Research Group (EPRG), University of Cambridge, UK*

Abstract

Zonal pricing with countertrading (a market-based redispatch) gives arbitrage opportunities to the power producers located in the export-constrained nodes. They can increase their profit by increasing the output in the day-ahead market and decrease it in the real-time market (the inc-dec game). We show that this leads to large inefficiencies in a standard zonal market. We also show how the inefficiencies can be significantly mitigated by changing the design of the real-time market. We consider a two-stage game with oligopoly producers, wind-power shocks and real-time shocks. The game is formulated as a two-stage stochastic equilibrium problem with equilibrium constraints (EPEC), which we recast into a two-stage stochastic Mixed-Integer Bilinear Program (MIBLP). We present numerical results for a six-node and the IEEE 24-node system.

Keywords: Two-stage game, Zonal pricing, Wholesale electricity market, Bilinear programming
JEL Classification: C61, C63, C72, D43, D47, L13, L94

[☆]Author names are listed alphabetically. This work is carried out by M. Sarfati under supervision of M.R. Hesamzadeh and in collaboration with P. Holmberg.

Mahir Sarfati was sponsored by the Swedish Centre for Smart Grids and Energy Storage (SweGRIDS). Pär Holmberg and Mahir Sarfati have been financially supported by the Jan Wallander and Tom Hedelius' Foundation, the Torsten Söderberg Foundation, and the Swedish Energy Agency.

Email addresses: mrhesamzadeh@ee.kth.se (M. R. Hesamzadeh), par.holmberg@ifn.se (P. Holmberg), sarfati@kth.se (M. Sarfati)

1. Introduction

Over the last two decades, a number of countries have deregulated their electricity industry in order to create competitive electricity markets. These markets have different methodologies to handle transmission congestion. The US and some other countries use nodal pricing while Europe and Australia have favored zonal pricing. Nodal pricing explicitly considers the transmission constraints and all accepted bids are paid with the local price in the node where the participant is located. Zonal pricing is an approximation of the nodal pricing regime, see Bjørndal et al. (2003). It aggregates specific nodes in order to create zones with uniform prices. Compared to nodal pricing, the zonal approximation would normally lead to a less efficient day-ahead dispatch. On the other hand, it could be argued that zonal pricing simplifies clearing of the day-ahead market and that it facilitates hedging and intra-day trading. Moreover, market participants, especially consumers, often favor zonal pricing.

In Europe, the zonal market is settled in two stages. We consider the version of the zonal market where all stages are market based, as in UK and the Nordic countries. The first settlement is the day-ahead market. In the economic dispatch related to the day-ahead market, each zone is assumed to be a copper plate and only transmission constraints between zones are considered. The second settlement is the real-time market, where all transmission constraints are fully represented in the economic dispatch problem. The simplified representation of transmission constraints in the day-ahead market may cause overloading of some of the transmission lines. This is relieved by counter-trading in the real-time market, the system operator accepts bids which reduce the production in the export constrained nodes and accepts bids which increase the production in the import constrained nodes.

Different representations of the transmission constraints in the two stages result in different prices in the two stages. This gives producers an arbitrage opportunity. Harvey and Hogan (2000a) and Harvey and Hogan (2000b) show that a producer in an export constrained node can increase its profit by selling more in the day-ahead market and then buy back power at a lower price in the real-time market. This kind of bidding behaviour is referred to as the *increase-decrease (inc-dec) game*. As explained by Alaywan et al. (2004) this game contributed to the electricity crisis in California and to that California and other markets in US switched from zonal to nodal pricing. According to Neuhoff et al. (2011), there are also problems with the inc-dec

game in the British electricity market. In this paper, we use simulations to quantify inefficiencies and other problems related with zonal pricing. We also show how these problems can be mitigated by a change in the design of the real-time market.

Several researchers have analyzed the zonally-priced electricity markets. Green (2007), Bjørndal and Jörnsten (2007) and Bjørndal et al. (2012) approximate the two stages by a one-stage game. Ruderer and Zöttl (2012) consider a regulated (non-market based) redispatch without the inc-dec game, as in the German electricity market. Holmberg and Lazarczyk (2015) study the strategic bidding under nodal, zonal and discriminatory pricing and concludes that even if the optimal dispatch of the generators are the same in all pricing approaches, the inc-dec game results in extra profit for the generators located at the export-constrained nodes. Holmberg and Lazarczyk (2015) disregard imperfect competition and focus on imperfections caused by arbitrage opportunities. Dijk and Willems (2011) consider both imperfect competition and arbitrage opportunities but their analysis is limited to two-node networks. They also show that the extra profit for export constrained producers distorts the investment signals and that this causes a long-run social welfare loss.

This paper contributes by studying oligopolistic competition of generators in zonally-priced electricity markets with multiple nodes. We assume that each producer chooses a bid price for its plant[1] and we consider three different methods to set prices in the real-time market: (1) pay-as-bid pricing as in Britain, (2) optimal zonal pricing and (3) a hybrid approach that approximates the Nordic market design. Optimal zonal pricing means that all constraints of the network are considered by the real-time market, but we add a set of extra constraints which require that the clearing price must be the same for all nodes within a zone. This is related to flow-based market coupling, which the European Union advocates for day-ahead markets, see Van den Bergh et al. (2016). Bjørndal et al. (2012) use optimal zonal pricing in order to approximate day-ahead markets. One of our contributions is that we evaluate how optimal zonal pricing works in the real-time market. This introduces an extra constraint in the real-time market, which normally makes

[1]In this paper, we consider a price-bid/Bertrand game. However, in principle our approach can be extended to the Cournot game (quantity-bid game) or price-quantity-bid game.

the design inefficient. On the other hand, this constraint also reduces price differences between the day-ahead and real-time market, which mitigates the inc-dec game. Overall, the market efficiency improves substantially in our examples, compared to standard zonal designs. In one of our examples, optimal zonal pricing is roughly as efficient as nodal pricing, which we use as a benchmark.

The uncertainty between the day-ahead and real-time markets is modeled by several scenarios. We formulate the two-stage price game as a two-stage stochastic Equilibrium Problem with Equilibrium Constraints (EPEC). The two-stage stochastic EPEC is reformulated as a two-stage stochastic MIBLP. We propose a solution algorithm which combines nonconvex generalized Benders decomposition (NGBD) algorithm, see Li et al. (2011), and the primal-relaxed dual (PRD) algorithm, which was applied by Floudas (2000). The proposed NGBD-PRD solution algorithm decomposes the two-stage stochastic MIBLP problem into a series of linear programs (LPs) and a mixed integer linear program (MILP). These LPs and MILP are solved iteratively until the ϵ-global solution is found. The computation time of the NGBD-PRD algorithm is reduced using parallelization and GAMS' multi-threading facility. The developed model and the proposed algorithm are demonstrated on a 6-node system and the IEEE 24-node example system for the alternative market designs that we consider.

The set of permissible price bids is discrete in our model. This means that we have the set of equilibria under control. Our solution algorithm can be programmed to solve for all equilibria, and we can verify that all best responses are global best responses.

The system operator makes sure that there is a feasible dispatch for any combination of bids. Thus similar to Willems (2002), we can avoid equilibrium ambiguities and the Generalized NE concept. These are well-known issues in Cournot games where the move of one player directly sets its own output and therefore constrains the permissible moves of other players in capacity constrained transmission networks, as explained by Stoft (1999).

Our method is related to Zhang and Xu (2013), who analyze numerical methods that can be used to solve for a two-stage stochastic EPEC. Zhang et al. (2010) use a Cournot model and Zhang and Kim (2010) a linear supply function equilibrium (SFE) model to study the strategic behaviour of generators that participate in a forward market and day-ahead market. Gupta et al. (2015) model the two-stage game in day-ahead and real-time markets for a radial three node network with nodal pricing. Hu and Ralph (2007)

analyze bilevel games for spot markets with nodal pricing.

This paper organized as follows: Section 2 formulates the two-stage game. The 6-node example system and the IEEE 24-node system are studied in detail in Section 3 and 4. Section 5 concludes the paper.

2. Mathematical Model (MIBLP)

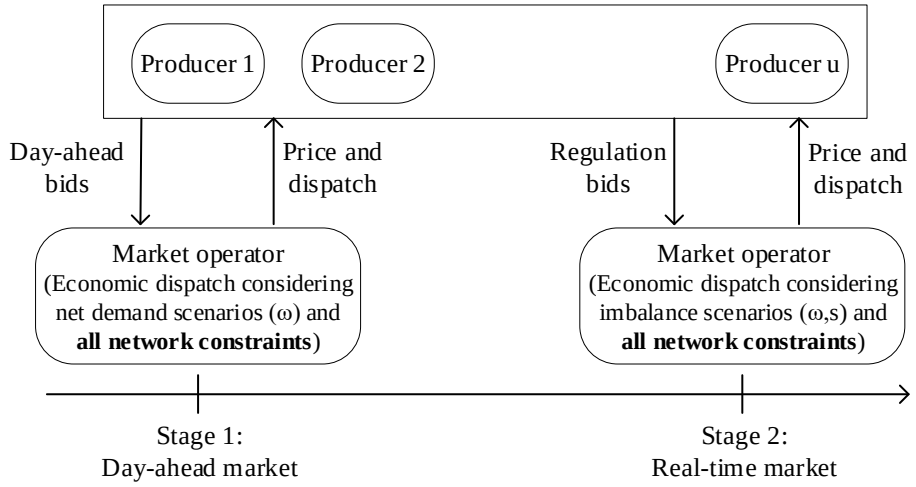

(a) Benchmark market design with nodal pricing

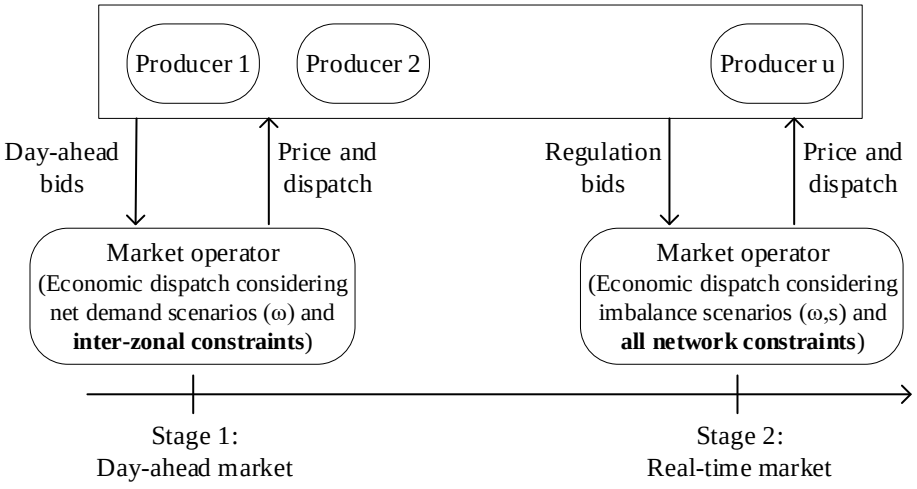

(b) Zonal market design in approaches 1, 2 and 3

Figure 1: The market designs considered in this study.

We consider a two-settlement electricity market which employs zonal pricing. The first settlement is the day-ahead market and the second one is the real-time market. We assume that both markets are physical and that oligopolistic producers participate in both markets. The zonal market design and its benchmark is illustrated in Fig. 1. The electricity market is modeled as a two-stage game under uncertainty. In the first stage, each generator chooses its day-ahead bid considering the presumed day-ahead decisions of its rivals and the Nash equilibrium in the real-time market. After generators submit their optimal day-ahead bids, the net-demand uncertainty (ω) is realized and revealed to the all generators. In the second stage, each generator chooses its regulation bids given the day-ahead dispatch results and the presumed regulation bids decisions of its rivals and submits it to the market operator. With the realized net-demand shock (s), the market operator clears the real-time market.

2.1. Nomenclature

Indices

u	Generator, $u = 1, ..., U$
n	Power system node, $n = 1, ..., N$
z	Zone, $z = 1, ..., Z$
k	Transmission line, $k = 1, ..., K$
l	Inter-zonal line, $l = 1, ..., L$
t	Index of Nash equilibria found, $t = 1, ..., T$
ω	Net demand scenario, $\omega = 1, ..., \Omega$
s	Net demand deviation scenario, $s = 1, ..., S$
a	Bidding action of generator, $a = 0, ..., A$

Parameters (upper-case letters)

$H_{k,n}$	PTDF matrix,
$H'_{l,z}$	Zonal PTDF matrix,
C_u	Marginal cost of unit u,
C_u^{up}	Marginal up-regulation cost of unit u,
C_u^{dn}	Marginal down-regulation cost of unit u,
G_u	Installed capacity of unit u,
F_k	Capacity of transmission line k,
$\bar{F}_l$	Capacity of inter-zonal line l,
$D_{n,\omega}$	Net demand at node n in scenario ω,
B_a	Step size of bidding action a,
$\bar{W}_{n,\omega,s}$	Wind production at node n,

$\Delta W_{n,\omega,s}$	Deviation in net demand at node n and scenario ω, s,
ξ_ω	Probability of scenario ω,
$\sigma_{\omega,s}$	Probability of scenario ω, s,
Ξ^μ,Ξ^β,Ξ^φ	Upper bound of Lagrange multiplier $\mu_{k,\omega,s}$, $\beta_{u,\omega,s}$, $\varphi_{u,\omega,s}$,
Variables (lower-case letters)	
x_u	Binary variable of day-ahead bidding decision of unit u,
$x^{up}_{u,\omega}, (x^{dn}_{u,\omega})$	Binary variable for up-regulation (down-regulation) bidding decision of unit u,
$\hat{c}_u$	Price bid of unit u,
$\hat{c}^{up}_{u,\omega}, (\hat{c}^{dn}_{u,\omega})$	Up-regulation (down-regulation) price bid of unit u in scenario ω,
$g_{u,\omega}$	Production level of unit u in scenario ω,
$g^{up}_{u,\omega,s}, (g^{dn}_{u,\omega,s})$	Up (down) regulation provided by unit u in scenario ω, s,
$v_{n,\omega,s}$	Wind spillage at node n in scenario ω, s,
$\rho_{n,\omega,s}, (p_{n,\omega})$	Real-time (day-ahead) market price at node n in scenario ω, s,
$\phi_{u,\omega,s}$	Real-time profit of unit u in scenario ω, s,
$\pi_{u,\omega}$	Day-ahead profit of unit u in scenario ω.

2.2. Competition in the real-time market

In this study, we consider three different pricing approaches in the real-time market which are summarized in Table 1. Approach 1 assumes that all accepted bids in the real-time market are paid their bid price as in the real-time market in Britain. In approach 2, the real-time market applies optimal zonal pricing, as in the day-ahead market by Bjørndal et al. (2012). This means that all constraints of the network are considered by the real-time market, but we add a set of extra constraints which require that the clearing price must be the same for all nodes within a zone. We assume that all accepted bids in the real-time market are paid with the marginal zonal price (MZP). One of our purposes with this pricing approach is that it should give similar prices as in the day-ahead market. This should reduce arbitrage opportunities and mitigate the inc-dec game. In approach 3, we determine the dispatch in a similar way as in approach 2. However, payments can differ. Similar to approach 2, the generators are paid the marginal price if the accepted regulation bid reduces the system imbalance. Otherwise they are paid with their bid price. The latter case indicates that the accepted bid is used to relieve congestion. Thus approach 3 is in-between approaches 1

and 2. Moreover, approach 3 is reminiscent of the real-time markets in the Nordic countries, where most bids are paid a zonal price, but bids that are accepted in the counter-trading process, which relaxes overloaded lines, are paid as bid.

Table 1: Real-Time pricing in the real-time market with zonal pricing, up-reg: Up-regulation, dn-reg: Down-regulation, PAB: Pay-as-bid, MZP: Marginal zonal price.

	Accepted bid					
System need	Approach 1		Approach 2		Approach 3	
	up-reg.	dn-reg.	up-reg.	dn-reg.	up-reg.	dn-reg.
up-reg.	PAB	PAB	MZP	MZP	MZP	PAB
dn-reg.	PAB	PAB	MZP	MZP	PAB	MZP

To find a Nash equilibrium in the two-stage game is a large-scale and complex problem. Solving this problem by exploring the entire solution space is normally not feasible, see Huppmann and Siddiqui (2018). To the best of our knowledge, no paper has attempted this for problems that are related to our study. Instead, the typical approach is to reduce the solution space by making the strategy set of bidders discrete as in Gabriel et al. (2013a), Gabriel et al. (2013b), Fuller and Celebi (2017), Huppmann and Siddiqui (2018) and Gabriel (2017). Similar to the these studies, we assume that the generators choose their regulation bids from a discrete set of permissible prices. In our model, each producer can choose a restricted number of prices which are related to the marginal cost of the producer. Each producer has unique costs and also a unique set of permissible prices. This means that there are no ties, and that we do not need a rationing rule.

2.2.1. Single generator's bidding problem in the real-time market

We want to solve for a subgame perfect Nash equilibrium (SPNE) in the two-stage game. Thus whatever happened in the first-stage, generators will play a Nash equilibrium in the second stage. It is most straightforward to solve for a SPNE backwards, so we start with the last stage, the real-time market. Each generator submits its up-regulation and down-regulation bids to the real-time market given the dispatch results in the day-ahead market. Moreover, we solve for a Nash equilibrium in the real-time market, so each generator chooses a bid that is a best response to the bids of its rivals in the real-time market. Hence, the strategic bidding decision of generator u in the

real-time market is formulated as a two-stage stochastic bilevel program in (1).

$$\underset{x^{up}_{u,a,\omega}, x^{dn}_{u,a,\omega}}{\text{Maximize}} \quad \mathbb{E}_{s|\omega}[\phi_{u,\omega,s}] \tag{1a}$$

Subject to:

$$\hat{c}^{up}_{u,\omega} = \sum_a B_a x^{up}_{u,a,\omega} C^{up}_u, \ \hat{c}^{dn}_{u,\omega} = \sum_a B_a x^{dn}_{u,a,\omega} C^{dn}_u \tag{1b}$$

$$x^{up}_{u,a,\omega}, x^{dn}_{u,a,\omega} \in \{0,1\} \tag{1c}$$

$$\text{where} \{g^{up}_{u,\omega,s}, g^{dn}_{u,\omega,s}, v_{n,\omega,s}\} \in \Bigg\{$$

$$\underset{g^{up}_{u,\omega,s}, g^{dn}_{u,\omega,s}, v_{n,\omega,s}}{\text{argMinimize}} \ \sum_{s,u} \sigma_{\omega,s} (\hat{c}^{up}_{u,\omega} g^{up}_{u,\omega,s} - \hat{c}^{dn}_{u,\omega} g^{dn}_{u,\omega,s}) \tag{1d}$$

Subject to:

$$\sum_u (g_{u,\omega} + g^{up}_{u,\omega,s} - g^{dn}_{u,\omega,s}) = \sum_n (v_{n,\omega,s} + D_{n,\omega} - \Delta W_{n,\omega,s}) : (\alpha_{\omega,s}) \ \forall \omega, s \tag{1e}$$

$$F_k - \sum_n H_{k,n} \Big(\sum_{n:u} (g_{u,\omega} + g^{up}_{u,\omega,s} - g^{dn}_{u,\omega,s}) - v_{n,\omega,s} - D_{n,\omega} + \Delta W_{n,\omega,s} \Big) \geq 0 : (\mu_{k,\omega,s}), \ \forall k, \omega, s \tag{1f}$$

$$0 \leq g^{up}_{u,\omega,s} \leq (G_u - g_{u,\omega}) : (\kappa_{u,\omega,s}, \beta_{u,\omega,s}) \ \forall u, \omega, s \tag{1g}$$

$$0 \leq g^{dn}_{u,\omega,s} \leq g_{u,\omega} : (\psi_{u,\omega,s}, \varphi_{u,\omega,s}) \ \forall u, \omega, s \tag{1h}$$

$$0 \leq v_{n,\omega,s} \leq \bar{W}_{n,\omega} + \Delta W_{n,\omega,s} : (\theta_{n,\omega,s}, \chi_{n,\omega,s}) \Bigg\} \tag{1i}$$

The up-regulation and the down-regulation price bids are modeled using binary variables in (1b). Here parameter B_a represents the mark-up (or mark-down) option in bidding action a. $g_{u,\omega}$ represents the given dispatch levels in the day-ahead market. The optimization problem (1d)-(1i) formulates the economic dispatch problem in the real-time market. The production cost is minimized in (1d) considering the energy balance constraint (1e), the transmission flow limits (1f), the capacity limits in (1g) and (1h) and the wind spillage limit (1i). The Lagrange multipliers related to each constraint are given in parenthesis. Since (1d)-(1i) is a linear program, the Karush-Kuhn-Tucker (KKT) conditions are both necessary and sufficient for a best response, which is shown by Gabriel et al. (2012). The complementary slackness condition is replaced by the strong duality conditions. The complementary slackness conditions are given by the product of inequality constraints and their related Lagrange multipliers should be equal to zero.

For example, the complementary slackness conditions for constraint $0 \leq g^{up}_{u,\omega,s}$ is $g^{up}_{u,\omega,s}\kappa_{u,\omega,s} = 0$. This is nonlinear due to the product of two continuous variables. The number of nonlinear terms increases with the number of the inequality constraints. However, when we replace the complementary slackness conditions by the strong duality condition, then we can avoid a large number of nonlinear constraints, and also represent them by a smaller number of linear constraints. This is explained in further detail in Appendix D. The stationary, dual feasibility and strong duality conditions of (1d)-(1i) are presented in (2a)-(2c),(2d) and (2e), respectively.

$$-\sigma_{\omega,s}\hat{c}^{up}_{u,\omega} + \alpha_{\omega,s} - \sum_{k,n:u} H_{k,n}\mu_{k,\omega,s} + \kappa_{u,\omega,s} - \beta_{u,\omega,s} = 0,\ \forall u,\omega,s \tag{2a}$$

$$\sigma_{\omega,s}\hat{c}^{dn}_{u,\omega} - \alpha_{\omega,s} + \sum_{k,n:u} H_{k,n}\mu_{k,\omega,s} + \psi_{u,\omega,s} - \varphi_{u,\omega,s} = 0,\ \forall u,\omega,s \tag{2b}$$

$$-\alpha_{\omega,s} + \sum_{k,n} H_{k,n}\mu_{k,\omega,s} + \theta_{n,\omega,s} - \chi_{n,\omega,s} = 0,\ \forall n,\omega,s \tag{2c}$$

$$\mu_{k,\omega,s}, \kappa_{u,\omega,s}, \beta_{u,\omega,s}, \psi_{u,\omega,s}, \varphi_{u,\omega,s}, \theta_{n,\omega,s}, \chi_{n,\omega,s} \geq 0 \tag{2d}$$

$$\begin{aligned}&\sigma_{\omega,s}\sum_{u}(-\hat{c}^{up}_{u,\omega}g^{up}_{u,\omega,s} + \hat{c}^{dn}_{u,\omega}g^{dn}_{u,\omega,s}) - (\alpha_{\omega,s}(\sum_{u} g_{u,\omega} + \sum_{n}(\Delta W_{n,\omega,s} - D_{n,\omega}))\\ &+ \sum_{u}\beta_{u,\omega,s}(G_u - g_{u,\omega}) + \sum_{u}\varphi_{u,\omega,s}g_{u,\omega} + \sum_{n}\chi_{n,\omega,s}(\bar{W}_{n,\omega} + \Delta W_{n,\omega,s})\\ &+ \sum_{k}\mu_{k,\omega,s}(F_k - \sum_{n} H_{k,n}(\sum_{n:u} g_{u,\omega} + \Delta W_{n,\omega,s} - D_{n,\omega}))) = 0,\ \forall\omega,s\end{aligned} \tag{2e}$$

Bidding decisions $\hat{c}^{up}_{u,\omega}$ and $\hat{c}^{dn}_{u,\omega}$ are defined using binary variables $x^{up}_{u,a,\omega}$ and $x^{dn}_{u,a,\omega}$ in (1b). Replacing (1d)-(1i) with its KKT conditions (2a)-(2e), we face two sets of bilinear terms in the resulting one-level program. These terms are: (i) $x^{up}_{u,a,\omega}g^{up}_{u,\omega,s}$ in (2e) and (ii) $x^{dn}_{u,a,\omega}g^{dn}_{u,\omega,s}$ in (2e). In this case the bilinear terms are the product of a binary and a continuous variable. Hence, they can be linearized using the McCormick reformulation, see Gupte et al. (2013). The McCormick reformulation is a technique for linearizing the bilinear terms. To explain the method, assume that we want to linearize $x^{up}_{u,a,\omega}g^{up}_{u,\omega,s}$. We first replace the bilinear term with a new variable $d_{u,a,\omega,s} = x^{up}_{u,a,\omega}g^{up}_{u,\omega,s}$ and then add the following linear constraints. These linear constraints are referred to as the McCormick envelopes for $x^{up}_{u,a,\omega}g^{up}_{u,\omega,s}$.

$$g^{up}_{u,\omega,s} + G_u(x^{up}_{u,a,\omega} - 1) \leq d_{u,a,\omega,s} \leq g^{up}_{u,\omega,s} \tag{3a}$$
$$0 \leq d_{u,a,\omega,s} \leq G_u x^{up}_{u,a,\omega} \tag{3b}$$

We derive the profit function of generator u in each real-time pricing approach. In approach 1, the generators are paid with their bid price in the real-time market. So the expected profit of generator u is:

$$\begin{aligned}\mathbb{E}_{s|\omega}[\phi_{u,\omega,s}] &= \sum_s \sigma_{\omega,s}((\hat{c}^{up}_{u,\omega} - C^{up}_u)g^{up}_{u,\omega,s} + C^{dn}_u g^{dn}_{u,\omega,s} - \hat{c}^{dn}_{u,\omega} g^{dn}_{u,\omega,s}) \\ &= \sum_s \sigma_{\omega,s}\big(\sum_a (B_a g^{up}_{u,\omega,s} x^{up}_{u,a,\omega} C^{up}_u) - C^{up}_u g^{up}_{u,\omega,s} + \\ &\quad C^{dn}_u g^{dn}_{u,\omega,s} - \sum_a (B_a g^{dn}_{u,\omega,s} x^{dn}_{u,a,\omega} C^{dn}_u)\big) \quad \forall u, \omega\end{aligned} \tag{4}$$

In approach 2, the market operator accepts the regulation bids such that nodal prices in each zone are equal to each other. Similar to the day-ahead model by Bjørndal et al. (2012), we mathematically model this by including the following constraints :

$$\sum_{n:z} \rho'_{z,\omega,s} = \rho_{n,\omega,s}, \forall n, \omega, s \tag{5a}$$
$$\sum_{u:z} \rho'_{z,\omega,s} \geq \hat{c}^{up}_{u,\omega} + (\overline{R}_{z,\omega,s} - 1)\Xi, \forall u, \omega, s \tag{5b}$$
$$\sum_{u:z} \rho'_{z,\omega,s} \leq \hat{c}^{dn}_{u,\omega} + (1 - \underline{R}_{z,\omega,s})\Xi, \forall u, \omega, s \tag{5c}$$

Here the notation $n : z$ represents the nodes which belongs to zone z, $\rho'_{z,\omega,s}$ represents the zonal price in zone z, and Ξ is a sufficiently large constant. The set of constraints (5) ensures a uniform price at the nodes inside the same zone. The parameter $\overline{R}_{z,\omega,s}$ is set to 1 if there is deficit of generation in zone z. Otherwise it is set to 0. Similarly, parameter $\underline{R}_{z,\omega,s}$ is set to 1 if there is excess of generation in zone z. Otherwise it is set to 0.

Adding a constraint involving dual variables as in (5) introduces a duality gap as in Ruiz et al. (2012). This means that, for given bids, the dispatch will be less optimal than nodal pricing. Hence, we change the right-hand side value of (2e) from 0 to $\bar{\epsilon}_{\omega,s}$. The calculation of parameter $\bar{\epsilon}_{\omega,s}$ will be explained in Appendix C. In approach 2, the generators are paid with the marginal zonal price in the real-time market. So the expected profit of generator u is:

$$\mathbb{E}_{s|\omega}[\phi_{u,\omega,s}] = \sum_s \sigma_{\omega,s}((\rho_{u,\omega,s} - C^{up}_u)g^{up}_{u,\omega,s} + (C^{dn}_u - \rho_{u,\omega,s})g^{dn}_{u,\omega,s}) \tag{6}$$

The real-time price faced by generator u can be written as in (7).

$$\rho_{u,\omega,s} = \sum_{u:n}(\alpha_{\omega,s} - \sum_{k} H_{k,n}\mu_{k,\omega,s})/\sigma_{\omega,s} \tag{7}$$

From (2a), (2b) and the complementary slackness conditions for (1g) and (1h), the profit in the real-time market in approach 2 is:

$$\mathbb{E}_{s|\omega}[\phi_{u,\omega,s}] = \sum_{s}(\beta_{u,\omega,s}(G_u - g_{u,\omega}) + \varphi_{u,\omega,s}g_{u,\omega}) + \sum_{s}\sigma_{\omega,s}(C^{dn}_u g^{dn}_{u,\omega,s} - \tag{8}$$

$$\sum_{a}(B_a g^{dn}_{u,\omega,s}x^{dn}_{u,a,\omega}C^{dn}_u)) + \sum_{s}\sigma_{\omega,s}(\sum_{a}(B_a g^{up}_{u,\omega,s}x^{up}_{u,a,\omega}C^{up}_u) - C^{up}_u g^{up}_{u,\omega,s}) \quad \forall u,\omega$$

The bilinear terms $g^{dn}_{u,\omega,s}x^{dn}_{u,a,\omega}$ and $g^{up}_{u,\omega,s}x^{up}_{u,a,\omega}$ in (4) and (8) are linearized using the McCormick reformulation.

Approach 3 has the same allocation mechanism as approach 2, but the transaction prices differ, which influences the profit function. In approach 3, the profit of generator u is a combination of (4) and (8). It can be calculated as follows:

$$\mathbb{E}_{s|\omega}[\phi_{u,\omega,s}] = \sum_{a,s}\sigma_{\omega,s}(C^{dn}_u g^{dn}_{u,\omega,s} - C^{up}_u g^{up}_{u,\omega,s} + (B_a g^{up}_{u,\omega,s}x^{up}_{u,a,\omega}C^{up}_u - \tag{9}$$

$$B_a g^{dn}_{u,\omega,s}x^{dn}_{u,a,\omega}C^{dn}_u)) + \sum_{a,s,z:u}(\overline{R}_{z,\omega,s}\beta_{u,\omega,s}(G_u - g_{u,\omega}) + \underline{R}_{z,\omega,s}\varphi_{u,\omega,s}g_{u,\omega}) \quad \forall u,\omega$$

We used the nodal pricing regime as a benchmark in our study. We model it as a zonal system with one node per zone so the profit function of the benchmark model is (8). Table 2 summarizes the two-stage stochastic model of each real-time pricing approach.

Table 2: The two-stage stochastic model in each real-time pricing approach, O.F.:Objective function, Cons: Constraints, M.E.: McCormick Envelopes.

	Approach 1 (MILP)	Approach 2 (MILP)	Approach 3 (MILP)	Benchmark (MILP)
O.F.	(1a)	(1a)	(1a)	(1a)
Cons.	(1b)-(1c)	(1b)-(1c)	(1b)-(1c)	(1b)-(1c)
	(1e)-(1i)	(1e)-(1i),(5)	(1e)-(1i),(5)	(1e)-(1i)
	(2a)-(2e),(4)	(2a)-(2e),(8)	(2a)-(2e),(9)	(2a)-(2e),(8)
	M.E. for $g^{up}_{u,\omega,s}x^{up}_{u,a,\omega}$, $g^{dn}_{u,\omega,s}x^{dn}_{u,a,\omega}$			

2.2.2. Nash equilibrium in the real-time market

The Nash equilibrium in the real-time market given the day-ahead dispatch decisions is found by solving all generators' real-time problems simultaneously. Since the regulation bids are discrete variables, the set $\{\hat{c}^{up,(1)}_{u,\omega},\hat{c}^{dn,(1)}_{u,\omega}, \hat{c}^{up,(2)}_{u,\omega}, \hat{c}^{dn,(2)}_{u,\omega},..., \hat{c}^{up,(I)}_{u,\omega},\hat{c}^{dn,(I)}_{u,\omega}\}$ is formed by different combinations of binary variables $x^{up}_{u,a,\omega}$, $x^{dn}_{u,a,\omega}$. Then the objective function of MILP model of each generator is replaced by:

$$\mathbb{E}_{s|\omega}[\phi_{u,\omega,s}] \geq \mathbb{E}_{s|\omega}[\phi^{(i)}_{u,\omega,s}] \quad \forall u, i, \omega \tag{10}$$

This transforms the MILP model of each generator to a set of mixed-integer linear constraints. The Nash equilibrium in the real-time market is found by solving the system of these mixed-integer linear constraints. We denote this system by $RTNE_\omega$.

2.3. Competition in the day-ahead market

In the day-ahead market, the generators choose their day-ahead bids from a discrete set of permissible prices. Similar to the real-time market, each producer has a unique set of permissible price bids. We consider cases where the market operator has set the flow limits between the zones for the day-ahead dispatch at a level which ensures security of the power system.

2.3.1. Single generator's bidding problem in the day-ahead market

We solve for a SPNE. Thus, generator u submits an optimal bid to the day-ahead market given the day-ahead bids of its rivals and considering the resulting Nash equilibrium in the real-time market.

$$\underset{\Lambda}{\text{Maximize}} \qquad \mathbb{E}_\omega[(p_{u,\omega} - C_u)g_{u,\omega} + \mathbb{E}_{s|\omega}[\phi_{u,\omega,s}]] \tag{11a}$$

Subject to:

$$\hat{c}_u = \sum_a B_a x_{u,a} C_u, \ (1b) \tag{11b}$$

$$x_{u,a}, x^{up}_{u,a,\omega}, x^{dn}_{u,a,\omega} \in \{0,1\} \tag{11c}$$

$$\text{where} \{p_{u,\omega}, g_{u,\omega}\} \in \left\{ \underset{g_{u,\omega}}{\text{argMinimize}} \sum_{u,\omega} \xi_\omega(\hat{c}_u g_{u,\omega}) \right. \tag{11d}$$

$$\sum_u g_{u,\omega} = \sum_n D_{n,\omega} \ : (\lambda_\omega) \ \forall\omega \tag{11e}$$

$$\bar{F}_l - \sum_z H'_{l,z}(\sum_{z:u,n} g_{u,\omega} - D_{n,\omega}) \geq 0 \ : (\gamma_{l,\omega}) \ \forall l, \omega \tag{11f}$$

$$0 \leq g_{u,\omega} \leq G_u \ : (\eta_{u,\omega}, \nu_{u,\omega}) \ \forall u, \omega \Big\} \tag{11g}$$

$$RTNE_\omega \ \forall \omega, \tag{11h}$$

where $\Lambda = \{\hat{c}_u,\ \hat{c}^{up}_{u,\omega},\ \hat{c}^{dn}_{u,\omega},\ x_{u,a},\ x^{up}_{u,a,\omega},\ x^{dn}_{u,a,\omega},\ g^{up}_{u,\omega,s},\ g^{dn}_{u,\omega,s},\ \mu_{k,\omega,s},\ \kappa_{u,\omega,s},\ \beta_{u,\omega,s},\ \psi_{u,\omega,s},\ \varphi_{u,\omega,s},\ \alpha_{\omega,s},\ \theta_{n,\omega,s},\ \chi_{n,\omega,s},\ \phi_{u,\omega,s},\ \phi^{(i)}_{u,\omega,s}\}$.

Equation (11b) models the price bids that generator u submitted to the day-ahead market. The expected total stated operation cost, which is based on producers' bids, is minimized in (11d) considering the energy balance constraint (11e), the inter-zonal transmission limits (11f) and generation limits (11g). Since problem (11d)-(11g) is a linear program, it is replaced by its equivalent KKT conditions.

After replacing $\alpha_{\omega,s} \sum_u g_{u,\omega}$ in (2e) with $\sum_n D_{n,\omega}$ from (11e), there are three sets of bilinear terms in (11). These are (i) $p_{u,\omega} g_{u,\omega}$ in (11a), (ii) $\hat{c}_u g_{u,\omega}$ in the strong duality condition of (11d-11g), (iii) $\sum_k H_{k,n} \mu_{k,\omega,s} g_{u,\omega}$, $\beta_{u,\omega,s} g_{u,\omega}$ and $\varphi_{u,\omega,s} g_{u,\omega}$ in (2e).

The day-ahead price is $p_{z,\omega} = (\lambda_\omega - \sum_l H'_{l,z} \gamma_{l,\omega})/\xi_\omega$. From the stationary condition for (11d-11g) and complementary slackness conditions for (11g), the profit function becomes as follows:

$$\mathbb{E}_\omega[\pi_{u,\omega}] = \sum_\omega \nu_{u,\omega} G_u + \sum_\omega \xi_\omega g_{u,\omega} C_u (\sum_a B_a x_{u,a} - 1), \ \forall u \tag{12}$$

Here the term $g_{u,\omega} x_{u,a}$ appears both in (12) and in the strong duality condition for (11d-11g). It is linearized using the McCormick reformulation as explained before. After this reformulation, the bilinear terms in (11) are $\sum_{k,n:u} H_{k,n} \mu_{k,\omega,s} g_{u,\omega}$, $\beta_{u,\omega,s} g_{u,\omega}$ and $\varphi_{u,\omega,s} g_{u,\omega}$. These bilinear terms are the product of two continuous variables. It is known that the exact linearization of this type of bilinearity is not possible, see for example Costa and Liberti (2012). Therefore, the resulting model for each generator is a MIBLP.

Our benchmark model is the nodal pricing model. Mathematically, the only difference to the zonal day-ahead model is that constraint (11f) is replaced by the constraint $(F_k - \sum_n H_{k,n}(\sum_{k:u,n} g_{u,\omega} - D_{n,\omega}) \geq 0)$.

2.3.2. Subgame Perfect NE in the two-stage game

The SPNE is found by solving all MIBLPs of generators simultaneously. Since each generator chooses its price bids from a finite set of choices, we

replace the objective function of the MIBLP model of each generator with (13).

$$\mathbb{E}_{\omega}[\pi_{u,\omega} + \mathbb{E}_{s|\omega}[\phi_{u,\omega,s}]] \geq \mathbb{E}_{\omega}[\pi^{(j),(i)}_{u,\omega} + \mathbb{E}_{s|\omega}[\phi^{(i)}_{u,\omega,s}]] \ \forall u, i, j \tag{13}$$

This transforms the MIBLP model to a set of mixed-integer bilinear constraints (MIBLCs). The Nash equilibrium of the two-stage bidding game is found by solving the MIBLCs of all generators together. This is formulated in (14) as an optimization problem. Inequality (13) is reformulated in (14c) by introducing the nonnegative slack variable ζ_u. The Nash equilibrium of the two-stage bidding game is found when ζ_u equals to 0. The two-stage bidding game is formulated in (14).

$$\underset{\Lambda'}{\text{Minimize}} \quad \sum_{u} \zeta_u \tag{14a}$$

$(11b), (11c), (12)$

KKT conditions of (11d)-(11g)

McCormick envelopes for $g_{u,\omega}x_{u,a}$

$RTNE_{\omega}\ \forall\omega$

$$\mathbb{E}_{\omega}[\pi_{u,\omega} + \mathbb{E}_{s|\omega}[\phi_{u,\omega,s}]] - \mathbb{E}_{\omega}[\pi^{(j),(i)}_{u,\omega} - \mathbb{E}_{s|\omega}[\phi^{(i)}_{u,\omega,s}]] + \zeta_u \geq 0, \ \forall u, i, j \tag{14b}$$

$$\zeta_u \geq 0, \ \forall u \tag{14c}$$

Problem (14) is a MIBLP and $\Lambda' = \Lambda \cup \{\pi^{(j),(i)}_{u,\omega}, p_{u,\omega}, g_{u,\omega}, \lambda_{\omega}, \gamma_{l,\omega}, \eta_{u,\omega}, \nu_{u,\omega}\}$.

2.4. Tackling Multiple Nash equilibria

The number of generators and the number of strategies available for each generator influences the existence and the number of Nash equilibria. In case of multiple Nash equilibria, the market outcomes may differ between different Nash equilibria, which would complicate the market analysis. This study uses two methodologies to tackle the multiple Nash equilibria.

Methodology 1: In methodology 1, we find all Nash equilibria. To do this, after we solve the model in (14) and find a Nash equilibrium, we add integer cut (C.5e) to remove the found Nash equilibrium from the solution space. This procedure is repeated until the objective value of (14) becomes a positive value. This means that no Nash equilibrium is left in the solution space.

Methodology 2: Large-scale examples require long computation times to solve the MIBLP model in (14), and it might not be practical to find all Nash equilibria. Another way of tackling multiple Nash equilibria is

to find the extremal (Worst/Best production cost) Nash equilibria as in Hesamzadeh and Biggar (2012). However, we have to modify their approach as we will apply methodology 2 to a problem that is much larger than in Hesamzadeh and Biggar (2012). We find a lower bound of the best production-cost Nash equilibrium and an upper bound of the worst production cost Nash equilibrium. Using the upper bound and the lower bound, we build an envelope which covers all Nash equilibria as in Hesamzadeh and Biggar (2013) (see Fig. 2). The lower bound of the envelope is calculated by total production cost when all generators bids their marginal costs to the both markets. The computation of the upper bound is explained in Appendix A. After finding the upper and the lower bound of the envelope, the interval between the upper bound and the lower bound is divided into subintervals with a tolerance (i.e. tolerance= $\frac{X_2 - X_1}{X_2}$). The MIBLP model in (14) is solved in each of these subintervals in a parallelized way, and a representative Nash equilibrium is found in each subinterval. This methodology enables us to find a set of representative Nash equilibria with a controlled tolerance.

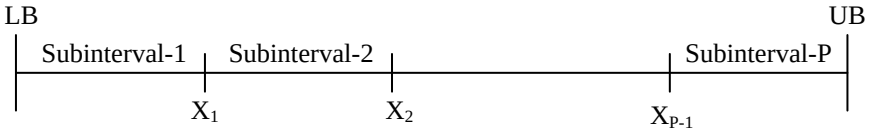

Figure 2: Equilibria envelope, LB: Lower bound of the best production cost Nash equilibrium, UB: Upper bound of the worst production cost Nash equilibrium, X_1: Upper limit of the subinterval-1.

One issue here is that there might not be a Nash equilibrium in every subinterval. We design a pre-feasibility-check method to find the subintervals which has no Nash equilibrium without solving the model in (14). The details of the pre-feasibility-check method is explained in Appendix B. Using this method, we identify the subintervals which has no Nash equilibrium, omit those subintervals, and then we compute the Nash equilibria.

2.5. Solution algorithm

The MIBLP model in (14) is a large scale model and it cannot be solved by the commercial MIBLP solvers in the GAMS environment. We solve the MIBLP model using a solution algorithm which is a combination of (i) the

nonconvex generalized Benders decomposition (NGBD) algorithm applied by Li et al. (2011) and (ii) the primal-relaxed dual (PRD) algorithm used by Floudas (2000).

It is computationally hard to solve a large scale Bilinear Program (BLP); it requires a long computation time. Thus our approach avoids BLP as much as possible. Our solution algorithm is an iterative process. We only report equilibria for our setting, but we use a McCormick relaxation McCormick (1976) when finding equilibrium candidates, i.e. we use a MILP relaxation of the MIBLP model when looking for equilibrium candidates. The resulting MILP model is easier to solve compared to the MIBLP model. The solution of the MILP model gives us a candidate SPNE. To ensure that the candidate equilibrium is a SPNE, the binary variables in the MIBLP model is fixed at their values in the candidate equilibrium and the obtained BLP model is solved. We reject candidates that are not SPNE for our setting. Once a solution has been found, we add an integer cut to make sure that a new candidate equilibrium is found in the next iteration. This process continues until a SPNE is found. In the 6-node example, we continue until all SPNE have been found. This approach means that we do not have to consider all possible combinations of binary variables, which would require us to solve the BLP model many times. The details of the solution algorithm can be found in the appendix C.

3. Illustrative Example

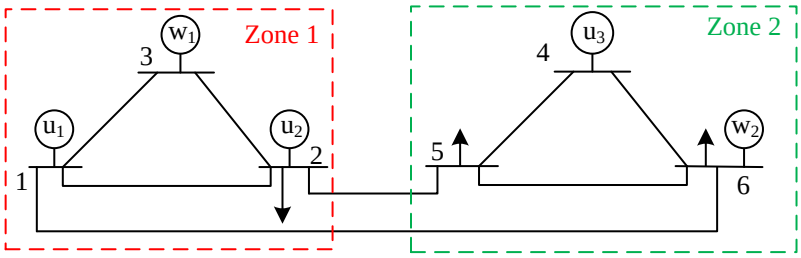

Figure 3: Single line diagram of 6-node example system, u_1,u_2, u_3: Conventional generators, W_1, W_2: Wind farms.

This section demonstrates the generators' bidding behaviors under different zonal pricing approaches for the 6-node that was used by Chao and Peck (1998). The considered time period is one hour. Fig. 3 shows the single line diagram of the illustrative example. We consider two zones. Zone

1 aggregates nodes 1, 2 and 3. Zone 2 aggregates nodes 4, 5 and 6. The 6-node example system has 3 competing generators u_1, u_2 and u_3 which are located at nodes 1, 2 and 4, respectively. The data related to the generators is presented in Table 3. The transmission capacity of the lines between nodes 1-2, 2-5 and 1-6 are set to 35 MW, 65 MW and 65 MW, respectively. The transmission capacity of the other lines is set to 100 MW. For the day-ahead market, the market operator sets the flow limit between zones 1 and 2 to 110 MW. The consumers located at nodes 2, 5 and 6 have fixed demand of 120 MW, 100 MW and 60 MW, respectively. Two wind farms are connected to nodes 3 and 6. Two wind generation scenarios are considered: 30 MW and 37.5 MW. In real-time, the deviation from the net demand ($\Delta W_{n,\omega,s}$) is modeled with 2 scenarios. Scenario s_1 represents the positive imbalance scenario ($\Delta W_{n,\omega,s_1} = 0.2W_{n,\omega}$), scenario s_2 represents the negative imbalance scenario ($\Delta W_{n,\omega,s_2} = -0.2W_{n,\omega}$). We assume that each generator has 3 bidding actions for day-ahead price bids with 0%, 10% mark-up and 10% mark-down. In real-time, the permissible up-regulation and down-regulation bids have 0%, 10%, 20% mark-up and 0%, 10%, 20% mark-down, respectively.

Table 3: Unit data for the 6-node system.

Unit	C ($/MWh)	C^{up} ($/MWh)	C^{dn} ($/MWh)	G_u (MW)
u_1	11.5	23	7.5	150
u_2	10.5	21	6.5	250
u_3	13	25	8.5	150

All generators submit their equilibrium bids ($\hat{c}_u$) to the day-ahead market. A short time before the delivery hour, units u_1, u_2 and u_3 consider the day-ahead dispatch results (including the wind power output) and submit their regulation bids to the real-time market. We use methodology 1 to tackle multiple Nash equilibria in this example. We report all Nash equilibria with different production costs. The SPNE for each market design is shown in Table 4. We observe that in approaches 1 and 3, u_1's down-regulation bid and u_2's up-regulation bid is accepted in all real-time scenarios (ω, s) due to the inc-dec game. That's why any combination of up/down-regulation bid of u_3, up-regulation bid of u_1 and down-regulation bid of u_2 is a Nash equilibrium. The dispatches and payoffs are the same in each one of these Nash equilibria, and therefore we only report one Nash equilibrium for approach 1 and 3 in Table 4. For approach 2 and the benchmark approach we found two Nash equilibria (A2-1 and A2-2) and three Nash equilibria (BA-1, BA-2 and BA-3),

Table 4: The SPNE for each approach and the expected profit of each generator, A1: Approach 1, A2: Approach 2, A3: Approach 3, BA: Benchmark approach, A2-1: First Nash equilibrium in approach 2, BA-1; First Nash equilibrium in the benchmark approach.

	u_1			u_2			u_3		
	$\hat{c}_u$	$(\hat{c}^{up}_{u,\omega},\hat{c}^{dn}_{u,\omega})$		$\hat{c}_u$	$(\hat{c}^{up}_{u,\omega},\hat{c}^{dn}_{u,\omega})$		$\hat{c}_u$	$(\hat{c}^{up}_{u,\omega},\hat{c}^{dn}_{u,\omega})$	
		ω_1	ω_2		ω_1	ω_2		ω_1	ω_2
A1	10.35	(23,6)	(23,6)	11.55	(25.2,5.2)	(25.2,5.2)	14.3	(30,7.65)	(30,7.65)
A2-1	12.65	(25.3,6)	(27.6,6)	11.55	(21,5.2)	(21,5.2)	14.3	(30,8.5)	(30,8.5)
A2-2	11.5	(23,7.5)	(27.6,7.5)	10.5	(21,5.2)	(21,5.2)	14.3	(30,8.5)	(30,8.5)
A3	10.35	(27.6,6)	(27.6,6)	11.55	(25.2,5.2)	(25.2,5.2)	14.3	(30,6.8)	(30,6.8)
BA-1	11.5	(27.6,6)	(25.3,6)	11.55	(25.2,5.2)	(25.2,5.85)	11.7	(30,6.8)	(27.5,6.8)
BA-2	11.5	(23,6)	(25.3,6)	11.55	(25.2,5.2)	(25.2,5.85)	11.7	(25,6.8)	(27.5,6.8)
BA-3	11.5	(23,6)	(23,6)	11.55	(25.2,6.5)	(25.2,6.5)	11.7	(25,8.5)	(25,8.5)

respectively.

Table 4 shows that in approaches 1 and 3, generator u_1 chooses a day-ahead bid which is lower than its marginal cost, which is consistent with an inc-dec strategy, see Harvey and Hogan (2000a). Table 5 presents further results that are consistent with the inc-dec game. It shows that the day-ahead dispatches in approaches 1 and 3 overload the intra-zonal line, line 1-2, by 32.1 MW in scenario ω_1 and by 34.6 MW in scenario ω_2. Here node 1 is the export-constrained node and node 2 is the import constraint node. To relieve this overloading, the market operator accepts u_1's down-regulation bid and u_2's up-regulation bid in every scenario. Accordingly, generator u_1 buys back in the real-time market and generator u_2 sells the energy, as reported in Table 5.

Table 5: Overloaded volume in the line 1-2 and the accepted counter-traded volume in the real-time market for A1 and A3, CT: Counter-traded volume.

Scenario ω	ω_1		ω_2	
Line 1-2 (MW)	32.1		34.6	
Scenario s	ω_1, s_1	ω_1, s_2	ω_2, s_1	ω_2, s_2
CT (MWh)	49.4	48.6	52.3	51.2

Table 6 shows that generator u_1 increases its total expected profit by at least eight times in approaches 1 and 3 compared to the benchmark approach (nodal pricing) due to the inc-dec game. Table 7 shows that producers' total

Table 6: The profit of each generator for each real-time pricing approach; , A1: Approach 1, A2: Approach 2, A3: Approach 3, BA: Benchmark approach, A2-1: First Nash equilbirium in approach 2, BA-1; First Nash equilibrium in the benchmark approach, $\Delta_u = \mathbb{E}_\omega[\pi_{u,\omega} + \mathbb{E}_{s|\omega}[\phi_{u,\omega,s}]]$, $\Phi_u = \mathbb{E}_\omega[\mathbb{E}_{s|\omega}[\phi_{u,\omega,s}]]$.

	π_u (\$/h)			Φ_u (\$/h)			Δ_u (\$/h)		
	u_1	u_2	u_3	u_1	u_2	u_3	u_1	u_2	u_3
A1	7.5	48.6	21.1	85.7	240	0	93.2	288.5	21.1
A2-1	0	206.1	21.1	0	21.4	27.1	0	227.5	48.2
A2-2	0	0	21.1	0	21.4	27.1	0	21.4	48.2
A3	7.5	48.6	21.1	111.5	316	0	93.2	288.5	21.1
BA-1	0	234.2	0	10.1	28.4	0	10.1	262.5	0
BA-2	0	234.2	0	10.1	21.6	0	10.1	255.8	0
BA-3	0	234.2	0	5.4	13.2	0	5.4	247.3	0

profits increase by 50-90%. Approach 2 is constructed to reduce the inc-dec game by setting the price in the day-ahead and real-time markets in a similar way, which reduces arbitrage opportunities. Indeed, we observe that in approach 2, the day-ahead dispatches do not overload any line in the network, when the generators bid their strategic day-ahead bids (A2) or their marginal costs (WALZ[2]) to the day-ahead market. This causes a significant decrease in the profit of u_1 in approach 2 compared to its profit in approaches 1 and 3. Similarly, we see in Table 7 that total profits for A2 is similar to the benchmark. Depending on equilibrium selection, A2 could even have significantly lower total profits compared to nodal pricing.

Table 7 shows the production cost in the day-ahead and real-time markets for each real-time pricing approach. We observe that approach 2 has a much lower production cost compared to approaches 1 and 3. The benchmark with nodal pricing has roughly the same production costs as approach 2.

Strategic bidding means that firms increase their profits by making statements of costs that do not correspond to their true costs. This leads to inefficiencies and higher (true) production costs. Depending on equilibrium selection, strategic bidding in approach 2 increases the production cost by 2-10% compared to case WALZ where all generators bids their true marginal cost. Similarly, the strategic bidding in the benchmark approach increases

[2]We define WALZ as a naive competitive equilibrium in market design A2 where the generators bid their true marginal costs to both day-ahead and real-time markets.

the production cost by 10% compared to the case WAL[3] where all generators bids their true marginal costs.

Table 7: The production cost and the total profit ($\sum_u \Delta_u$) for each market design. PC^{DA}: The production cost in the day-ahead dispatch ($/h), PC^{RT}: The production cost in the real-time dispatch ($/h), TPC: The total production cost ($/h), WAL: Naive competitive bidding in BA, WALZ: Naive competitive bidding in A2.

	PC^{DA}	PC^{RT}	TPC	$\sum_u \Delta_u$
WAL	2232.64	104.43	2337.07	0.56
WALZ	2271.88	101.29	2373.17	15.72
A1	2319.06	1096.96	3416.02	402.85
A2-1	2499.06	119.05	2618.11	275.69
A2-2	2293.56	119.05	2412.61	69.62
A3	2319.06	1096.96	3416.02	504.68
BA-1	2449.33	129.6	2578.93	272.65
BA-2	2449.33	126.06	2575.39	265.9
BA-3	2449.33	120.08	2569.41	252.76

In this example system, each generator has 3x3=9 (3 up-regulation, 3 down-regulation) strategies for each scenario ω. We consider 2 net-demand scenarios in the day-ahead market, so each generator has 9x9=81 possible strategies when deciding on the real-time bid. Each generator also has three possible strategies for its day-ahead bid. Thus, in the two-stage game, each generator has 81x3=243 possible strategies. Since we have 3 generators in the example system, the total number of bid combinations is 14,348,907. If we iterate over each of these combinations and each solution takes hypothetically 1 second, the computation of the SPNE will take approximately 166 days. However our solution algorithm can compute the SPNE in moderate time by first using a MILP model to identify equilibrium candidates, which are then evaluated in detail.

[3]We define WAL as a naive competitive equilibrium in the benchmark market design where the generators bid their true marginal costs to both day-ahead and real-time markets.

4. IEEE 24-node example system

An original version of the IEEE 24-node example system is presented by Grigg et al. (1999). In this subsection we modify this example somewhat and use it to demonstrate our zonal pricing models and the proposed solution algorithm in a larger system. We consider three zones. Zone 1 aggregates nodes 15-23. Zone 2 aggregates nodes 11-14 and 24. Zone 3 aggregates nodes 1-10. The transmission capacity of the lines between nodes 1-2, 3-24, 14-16 and 21-22 are set to 200 MW, 175 MW, 200 MW and 425 MW, respectively. For the day-ahead market, the market operator sets the flow limits between zones 1 and 2 to 400 MW and between zones 2 and 3 to 820 MW. The data related to the generators is presented in Table 8.

Table 8: Unit data for 24-node system.

Unit	node	C ($/MWh)	C^{up} ($/MWh)	C^{dn} ($/MWh)	G_u (MW))
u_1	1	19	27	11	500
u_2	2	15.5	23.5	11.5	400
u_3	13	14.5	22.5	9.5	600
u_4	21	13	20.5	7	1200
u_5	22	13.5	21.5	8.5	1100

Table 9: The net demand deviation scenarios.

	s_1	s_2	s_3	s_4	s_5	s_6
$\Delta W_{n,\omega_1,s}$ (MWh)	51.3	42.75	34.2	25.65	17.1	0
	s_7	s_8	s_9	s_{10}	s_{11}	
$\Delta W_{n,\omega_1,s}$ (MWh)	-17.1	-25.65	-34.2	-42.75	-51.3	

Five wind farms are connected to nodes 8, 11, 12, 16 and 23. One wind generation scenario (171 MW) is considered. The deviation from the net demand is modeled with 11 scenarios shown in Table 9. Scenario s_1, s_2, s_3, s_4, and s_5 represent the positive imbalance scenarios, scenario s_6 represents the no imbalance scenario and scenarios s_7, s_8, s_9, s_{10}, and s_{11} represent the negative imbalance scenario. We assume that each generator has 3 bidding actions for day-ahead price bids: 0%, 10% mark-up and 10% mark-down. For up- and down-regulation bids in the real-time market, we allow for 0%, 10%, 20% mark-up and 0%, 10%, 20% mark-down, respectively.

Table 10: SPNE in the subintervals, SI: Subinterval, TPC: Total production cost ($/h), Fail: Failed from pre-feasibility check, no SPNE: Passed from pre-feasibility check but no SPNE found by the solution algorithm.

SI#	TPC interval	A1	A2	A3	TPC interval	BA
SI1	28492.6-31342	no SPNE	**SPNE**	no SPNE	28502.7-31353	**SPNE**
SI2	31342-34476	**SPNE**	Fail	**SPNE**	31353-34488	Fail
SI3-SI10	34476-73903	Fail	Fail	Fail	34488-73929	Fail

We apply methodology 2 to tackle multiple Nash equilibria. The lower and upper bound of the envelope is calculated as 28492.6 $/h and 73903 $/h for A1, A2 and A3 and 28502.7 $/h and 73929 $/h for BA. We split the envelops in 10 subintervals by setting the tolerance as 10%. Table 10 shows that, according to the pre-feasibility check, there are no SPNE in subintervals between SI3 and SI10 for A1 and A3. Using our solution algorithm we solve the SPNE model in (14) for subinterval-1 and subinterval-2. For A1 and A3, we find a representative Nash equilibrium in SI2, but not in SI1. For A2 and BA, all subintervals between SI2 and SI10 fails in the pre-feasibility check, and we find a representative Nash equilibrium in SI1.

Table 11: The SPNE in each approach, A1: Approach 1, A2: Approach 2, A3: Approach 3, BA: Benchmark approach, $\hat{c}_u$: Day-ahead price bid ($/MWh), $(\hat{c}_u^{up}, \hat{c}_u^{dn})$: Up and down regulation price bid ($/MWh,$/MWh).

		u_1	u_2	u_3	u_4	u_5
A1	$\hat{c}_u$	20.9	17.05	15.95	14.3	12.15
	$(\hat{c}_u^{up}, \hat{c}_u^{dn})$	(32.4,8.8)	(28.2,9.2)	(24.75,7.6)	(24.6,5.6)	(23.65,6.8)
A2	$\hat{c}_u$	20.9	17.05	15.95	14.3	14.85
	$(\hat{c}_u^{up}, \hat{c}_u^{dn})$	(32.4,9.9)	(23.5,11.5)	(22.5,9.5)	(20.5,5.6)	(21.5,8.5)
A3	$\hat{c}_u$	20.9	17.05	15.95	14.3	12.15
	$(\hat{c}_u^{up}, \hat{c}_u^{dn})$	(32.4,9.9)	(25.85,10.35)	(22.5,7.6)	(24.6,6.3)	(23.65,6.8)
BA	$\hat{c}_u$	20.9	15.50	15.95	14.3	13.5
	$(\hat{c}_u^{up}, \hat{c}_u^{dn})$	(32.4,9.9)	(25.85,10.35)	(27,8.55)	(24.6,6.3)	(23.65,6.8)

Table 11 shows that in approaches 1 and 3, u_5 chooses a day-ahead bid which is lower than its marginal cost and becomes the cheapest generator in the market. We observe in Table 12 that the day-ahead dispatches in approaches 1 and 3 overload the intra-zonal line between nodes 21 and 22 by 233.78 MW. To relieve this overloading, the volumes reported in Table 12

are counter-traded in the real-time market. Generators u_3, u_4 and u_5 provide the necessary up-regulation (u_3, u_4) and down-regulation (u_5) for counter-trading. In contrast, we observe that no transmission line is overloaded when the generators bid their strategic day-ahead bids (A2) or their marginal costs (WALZ) to the day-ahead market when there is optimal zonal pricing in the real-time market. Table 13 shows that u_4 increases its total profit by 114% in A1 and by 335% in A3 compared to the benchmark approach. Moreover u_5 increases its profit by 20.6 times in A1 and by 21.9 times in A3, compared to the benchmark approach.

Table 12: Overloading volume for the line between nodes 21 and 22 and the volume of accepted regulation bids for counter-trading (CT) in each scenario in A1 and A3.

Line 21-22 (MWh)	233.78					
	s_1	s_2	s_3	s_4	s_5	s_6
CT (MWh)	133.69	172.63	211.57	250.51	289.45	367.33
	s_7	s_8	s_9	s_{10}	s_{11}	
CT (MWh)	359.71	356.58	354.52	352.46	350.94	

Table 13: The profit of each generator in each real-time pricing approaches; π_u (\$/h): Profit in the day-ahead market, Φ_u (\$/h): Expected profit in the real-time market, Δ_u (\$/h): Total profit in both markets.

	A1					A2				
	u_1	u_2	u_3	u_4	u_5	u_1	u_2	u_3	u_4	u_5
π_u	0	520.8	778.65	22.1	880	0	520.8	778.65	1452.1	0
Φ_u	7	64.9	59.62	1327.38	621.1	9.54	230.79	427.9	406.26	31.51
Δ_u	7	585.7	838.27	1349.48	1501.1	9.54	751.59	1206.55	1858.36	31.51
	A3					BA				
	u_1	u_2	u_3	u_4	u_5	u_1	u_2	u_3	u_4	u_5
π_u	0	520.8	778.65	22.1	880	0	739.35	556.9	597.31	0
Φ_u	7	122.9	283.5	2714.1	713.54	3.65	43.52	342.48	32.26	69.59
Δ_u	7	643.7	1062.15	2736.2	1593.54	3.65	782.87	899.38	629.57	69.59

Table 14 illustrates that approach 2 has the lowest production cost and approaches 1 and 3 have the highest production cost among the zonal market designs. The strategic bidding in approach 2 increases the production cost by 9.7% compared to case WALZ where all generators bids their true marginal

cost. Similarly, the strategic bidding in the benchmark approach increases the production cost by 6.9% compared to case WAL where all generators bids their true marginal costs. In this example, the total profit of generators is lower in approach 2 in comparison to approach 1 and 3, but it is significantly higher than the benchmark approach.

Table 14: The production cost and the total profit ($\sum_u \Delta_u$) in each market designs, PC^{DA}: The production cost in the day-ahead dispatch, PC^{RT}: The production cost in the real-time dispatch, TPC: The total production cost, WAL: Naive competitive bidding in BA, WALZ: Naive competitive bidding in A2.

	PC^{DA} ($/h)	PC^{RT} ($/h)	TPC ($/h)	$\sum_u \Delta_u$ ($/h)
WAL	27480.38	1022.33	28502.71	122.97
WALZ	27515.5	977.1	28492.6	577.45
A1	27902.05	6567.12	34469.17	4281.56
A2	30267.05	989.65	31256.7	3857.54
A3	27902.05	6455.82	34357.87	6042.59
BA	28973.54	1417.74	30391.28	2385.07

5. Conclusion

This paper applies a two-stage game to study oligopolistic competition of generators in zonally-priced electricity markets with a day-ahead and a real-time market. The two-stage game is mathematically formulated as a two-stage stochastic EPEC and it is recast into a two-stage stochastic MIBLP. The developed model is solved using a combination of the nonconvex generalized Benders decomposition and the primal relaxed-dual algorithms. Our solution algorithm decomposes the MIBLP problem into a series of a mixed-integer linear program and linear programs and solves them iteratively. The developed two-stage stochastic MIBLP model and the NGBD-PRD solution algorithm are demonstrated on the 6-node and IEEE 24-node example systems.

Our numerical results illustrate that the inc-dec game can lead to large production inefficiencies and large profits for producers in zonal electricity markets in comparison to nodal pricing. However, our results also illustrate how the inc-dec game can be mitigated by modifying the design of the real-time market, such that price differences within a zone are minimized. This

extra constraint in the real-time market would normally introduce welfare losses. On the other hand the extra constraint means that prices in the day-ahead and real-time market are set in a more similar way, which reduces the arbitrage opportunities. This mitigates the inc-dec game and the excess profits associated with this game.

Appendix A. Calculating the upper bound of the Nash equilibria envelope

To find the upper bound of the envelope, objective function (14a) and constraint (14c) in model (14) are replaced by (A.1) and (13), respectively.

$$\text{Maximize} \sum_{s,u} \sigma_{\omega,s}(\hat{c}^{up}_{u,\omega} g^{up}_{u,\omega,s} - \hat{c}^{dn}_{u,\omega} g^{dn}_{u,\omega,s}) + \sum_{u,\omega} \xi_{\omega}(\hat{c}_u g_{u,\omega}) \tag{A.1}$$

Moreover the bilinear terms $\sum_{k,n:u} H_{k,n}\mu_{k,\omega,s} g_{u,\omega}$, $\sum_u \beta_{u,\omega,s} g_{u,\omega}$ and $\sum_u \varphi_{u,\omega,s} g_{u,\omega}$ in (14) are replaced by $\tau_{u,\omega,s}$, $\hat{\tau}_{u,\omega,s}$ and $\bar{\tau}_{u,\omega,s}$ which is bounded through constraints (C.1), (C.2), (C.3), respectively. This transforms the MIBLP model in (14) into a MILP model. The solution of the resulting MILP model gives the upper bound of the envelope.

Appendix B. Pre-feasibility check method

Our method is based on two properties of the duality: (i) The dual of a nonconvex problem is always a convex problem Boyd and Vandenberghe (2004) and (ii) if a problem is infeasible, the dual of this problem is unbounded Boyd and Vandenberghe (2004). To use these properties, we formulate the problem based on (14) by replacing $\sum_u \zeta_u$ in (14a) by $\sum_{\omega,s} \hat{\epsilon}_{\omega,s}$ and replacing (14c) by (13). The resulting problem is a MIBLP and it is infeasible if there is no Nash equilibrium in a given subinterval. Instead of solving nonconvex MIBLP, we relaxed the integrality constraints of the binary variables and take the dual of it. The dual problem is an LP model and it is easier to solve compared to the MIBLP. We solve the dual problem in each subinterval. We may face two cases: (i) if the dual problem has a finite solution, there might be a Nash equilibrium in this subinterval or (ii) if the dual problem is unbounded, there is no Nash equilibrium in this subinterval. Using this method, we identify the subintervals which has no Nash equilibrium and reduce the number of subintervals we search for the Nash equilibrium. Note that due to the nonconvexity of the MIBLP, in some subintervals we may have a finite dual solution but there might not be a Nash

equilibrium. However if the dual solution is unbounded, it is guaranteed that there is no Nash equilibrium in a subinterval.

Appendix C. Solution Algorithm

The MIBLP model in (14) is solved by a combination of (i) the nonconvex generalized Benders decomposition (NGBD) algorithm Li et al. (2011) and (ii) the primal-relaxed dual (PRD) algorithm Floudas (2000). The NGBD algorithm first decomposes the MIBLP model into MILP and BLP models. The MILP model is solved by a standard Benders decomposition algorithm by iterating between the relaxed MILP (RMILP) model and LP model. To ensure the ϵ-global solution for the MIBLP, the BLP model needs to be solved to ϵ-global solution. The BARON Tawarmalani and Sahinidis (2005) solver in GAMS can solve a BLP problem to ϵ-global optimum. In our tests, the BARON solver can solve the BLP model in small-scale case studies. However, it cannot return any solution in larger case studies. Therefore, we use the parallelized PRD algorithm to solve the large scale BLP models. The PRD algorithm solves the BLP model by iterating between lower-bound and upper-bound LPs. The concept of the NGBD-PRD algorithm is shown in Fig. C.4.

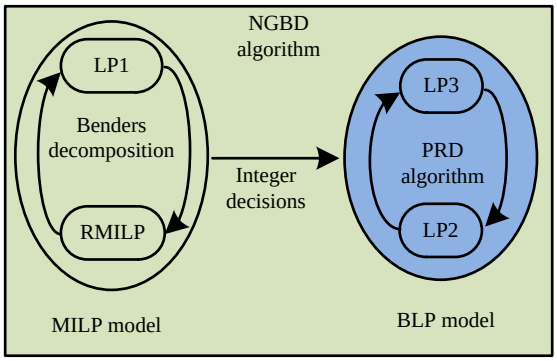

Figure C.4: The concept of the NGBD-PRD algorithm.

Appendix C.1. MILP model

The MILP model finds a lower bound of the MIBLP problem. Using McCormick relaxation McCormick (1976), the bilinear terms $\sum_{k,n:u} H_{k,n}\mu_{k,\omega,s}g_{u,\omega}$, $\sum_u \beta_{u,\omega,s}g_{u,\omega}$ and $\sum_u \varphi_{u,\omega,s}g_{u,\omega}$ in (14) are replaced by $\tau_{u,\omega,s}$, $\hat{\tau}_{u,\omega,s}$ and $\bar{\tau}_{u,\omega,s}$

which is bounded through constraints (C.1), (C.2), (C.3), respectively. We denote $\sum_{k,n:u} H_{k,n}\mu_{k,\omega,s}$ by $\hat{\mu}_{u,\omega,s}$ in constraints (C.1). This transforms the MIBLP model into a MILP problem. This MILP problem is solved using benders decomposition which iterates between a relaxed MILP model (RMILP) and a LP model (LP1).

$$\Xi^{\mu} g_{u,\omega} + G_u(\hat{\mu}_{u,\omega,s} - \Xi^{\mu}) \leq \tau_{u,\omega,s} \leq \Xi^{\mu} g_{u,\omega},\ \forall u,\omega,s$$
$$0 \leq \tau_{u,\omega,s} \leq G_u \hat{\mu}_{u,\omega,s},\ \forall u,\omega,s \tag{C.1}$$
$$\Xi^{\beta} g_{u,\omega} + G_u(\beta_{u,\omega,s} - \Xi^{\beta}) \leq \hat{\tau}_{u,\omega,s} \leq \Xi^{\beta} g_{u,\omega},\ \forall u,\omega,s$$
$$0 \leq \hat{\tau}_{u,\omega,s} \leq G_u \beta_{u,\omega,s},\ \forall u,\omega,s \tag{C.2}$$
$$\Xi^{\varphi} g_{u,\omega} + G_u(\varphi_{u,\omega,s} - \Xi^{\varphi}) \leq \bar{\tau}_{u,\omega,s} \leq \Xi^{\varphi} g_{u,\omega},\ \forall u,\omega,s$$
$$0 \leq \bar{\tau}_{u,\omega,s} \leq G_u \varphi_{u,\omega,s},\ \forall u,\omega,s \tag{C.3}$$

Appendix C.1.1. LP1 model

By fixing the integer variables the MILP becomes an LP. This LP is obtained by adding constraint (C.4) to the MILP.

$$\tilde{\boldsymbol{b}} = \bar{\boldsymbol{b}} : (\boldsymbol{\delta}) \tag{C.4}$$

Vector $\bar{\boldsymbol{b}}$=[$\bar{x}_{u,a}$ $\bar{x}^{up}_{u,a,\omega}$ $\bar{x}^{dn}_{u,a,\omega}$] is the given integer decisions and vector $\tilde{\boldsymbol{b}}$=[$\tilde{x}_{u,a}$ $\tilde{x}^{up}_{u,a,\omega}$ $\tilde{x}^{dn}_{u,a,\omega}$] includes continuous variables. The objective value of the subproblem (Υ) gives the upper bound of the MILP problem. If this problem is infeasible, the feasibility subproblem is formulated and solved as in Li et al. (2011).

Appendix C.1.2. LP1-R model

In the real-time pricing approaches 2 and 3, the duality gap ($\bar{\epsilon}_{\omega,s}$) in the LP1 model is nonzero. To calculate the minimum $\bar{\epsilon}_{\omega,s}$ for the LP1 model, the LP1-R model is solved. To obtain the LP1-R model, constraints (10) and (13) are removed from the LP1 model and the objective function is changed to minimize $\sum_{\omega,s} \hat{\epsilon}_{\omega,s}$. The optimal value of $\hat{\epsilon}_{\omega,s}$ in the LP1-R model is fixed in the LP1 model.

Appendix C.1.3. RMILP model

Given the Lagrange multipliers for the subproblem in iteration y, $\boldsymbol{\delta}^{(y)}$=[$\delta^{(y)}_{u,a}$ $\delta^{up,(y)}_{u,a,\omega}$ $\delta^{dn,(y)}_{u,a,\omega}$], we formulate the master problem in (C.5).

$$\text{Minimize} \quad \varrho \tag{C.5a}$$
$$\text{Subject to}$$
$$\varrho \geq \Upsilon^{(e)} + \boldsymbol{\delta}^{(e)}(\boldsymbol{b} - \bar{\boldsymbol{b}}^{(e)}),\ \forall e \in E^y \tag{C.5b}$$
$$0 \geq \Upsilon^{(l)} + \boldsymbol{\delta}^{(l)}(\boldsymbol{b} - \bar{\boldsymbol{b}}^{(l)}),\ \forall l \in O^y \tag{C.5c}$$
$$\sum_{r:\boldsymbol{b}=1} \boldsymbol{b}_r^{(y)} - \sum_{r:\boldsymbol{b}=0} \boldsymbol{b}_r^{(y)} \leq |r| - 1,\ \forall y \in E^y \cup O^y \tag{C.5d}$$
$$\sum_{r:\boldsymbol{b}=1} \boldsymbol{b}_r^{(t)} - \sum_{r:\boldsymbol{b}=0} \boldsymbol{b}_r^{(t)} \leq |r| - 1,\ \forall t \tag{C.5e}$$
$$\varrho \geq \underline{\varrho} \tag{C.5f}$$

Here vector $\boldsymbol{b}$=$[x_{u,a}\ x^{up}_{u,a,\omega}\ x^{dn}_{u,a,\omega}]$ represents the integer decisions. Constraint (C.5b) is the optimality cut in iteration e and $\forall e \in E^y$. Constraint (C.5c) is the feasibility cut in iteration l and $\forall l \in O^y$. Constraints (C.5d) and (C.5e) are the integer cuts which forbids a known integer solution to be considered again. Constraint (C.5f) models the lower bound of ϱ.

Appendix C.2. BLP model

The BLP model is constructed by fixing the integer variables to a given value in the MIBLP model. We use the PRD algorithm to compute the ϵ-global solution of the BLP model. The PRD algorithm decomposes the BLP model into two linear models (LP2 model and LP3 model) and solves them iteratively.

Appendix C.2.1. LP2 model

To obtain the LP2 model, we fix $g_{u,\omega}$ in bilinear terms $\sum_{k,n:u} H_{k,n}\mu_{k,\omega,s}g_{u,\omega}$, $\sum_u \beta_{u,\omega,s}g_{u,\omega}$ and $\sum_u \varphi_{u,\omega,s}g_{u,\omega}$ in the BLP model. The objective value of the LP2 model (Ψ) provides a valid upper bound of the BLP problem. If the value of $g_{u,\omega}$ in iteration M ($\bar{g}^{(M)}_{u,\omega}$) makes the LP2 model infeasible, the feasibility model LP2 is formulated and solved as in Floudas (2000).

Appendix C.2.2. LP2-R model

To calculate the minimum $\bar{\epsilon}_{\omega,s}$ for the LP2 model, the LP2-R model is solved. To obtain the LP2-R model, constraints (10) and (13) are removed from the LP2 model and the objective function is changed to minimize $\sum_{\omega,s} \hat{\epsilon}_{\omega,s}$. The optimal value of $\hat{\epsilon}_{\omega,s}$ in the LP2-R model is fixed in the LP2 model.

Appendix C.2.3. LP3 model

The LP3 model finds a lower bound of the BLP problem. In each iteration of the PRD algorithm a linearized Lagrangian is added to the LP3 model and the lower bound of the BLP problem is updated. Given the Lagrange multipliers of LP2 model (vector $\boldsymbol{\Theta}^{(M)}$) and the optimal values of all variables except the ones in the bilinear terms in LP2 (vector $\mathbf{Y}^{(M)}$), the linearized Lagrangian is formulated in (C.6a). Vectors $\boldsymbol{\mu}$, $\boldsymbol{\beta}$ and $\boldsymbol{\varphi}$ denote variables $\mu_{k,\omega,s}$, $\beta_{u,\omega,s}$ and $\varphi_{u,\omega,s}$, respectively.

$$L(\boldsymbol{\mu},\boldsymbol{\beta},\boldsymbol{\varphi},g_{u,\omega},\mathbf{Y}^{(M)},\boldsymbol{\Theta}^{(M)})|^{lin}_{\boldsymbol{\mu}^{(M)},\boldsymbol{\beta}^{(M)},\boldsymbol{\varphi}^{(M)}} = \sum_{k,\omega,s} h^{(M)}_{k,\omega,s}(g_{u,\omega})(\boldsymbol{\mu}-\boldsymbol{\mu}^{(M)})+$$
$$\sum_{u,\omega,s} \hat{h}^{(M)}_{u,\omega,s}(g_{u,\omega})(\boldsymbol{\beta}-\boldsymbol{\beta}^{(M)}) + \sum_{u,\omega,s} \tilde{h}^{(M)}_{u,\omega,s}(g_{u,\omega})(\boldsymbol{\varphi}-\boldsymbol{\varphi}^{(M)})+$$
$$L(\boldsymbol{\mu}^{(M)},\boldsymbol{\beta}^{(M)},\boldsymbol{\varphi}^{(M)},g_{u,\omega},\mathbf{Y}^{(M)},\boldsymbol{\Theta}^{(M)}) \tag{C.6a}$$
$$h^{(M)}_{k,\omega,s}(g_{u,\omega}) = \nabla_{\boldsymbol{\mu}} L(\boldsymbol{\mu},\boldsymbol{\beta},\boldsymbol{\varphi},g_{u,\omega},\mathbf{Y}^{(M)},\boldsymbol{\Theta}^{(M)}) \tag{C.6b}$$
$$\hat{h}^{(M)}_{u,\omega,s}(g_{u,\omega}) = \nabla_{\boldsymbol{\beta}} L(\boldsymbol{\mu},\boldsymbol{\beta},\boldsymbol{\varphi},g_{u,\omega},\mathbf{Y}^{(M)},\boldsymbol{\Theta}^{(M)}) \tag{C.6c}$$
$$\tilde{h}^{(M)}_{u,\omega,s}(g_{u,\omega}) = \nabla_{\boldsymbol{\varphi}} L(\boldsymbol{\mu},\boldsymbol{\beta},\boldsymbol{\varphi},g_{u,\omega},\mathbf{Y}^{(M)},\boldsymbol{\Theta}^{(M)}) \tag{C.6d}$$

Where $L(\boldsymbol{\mu},\boldsymbol{\beta},\boldsymbol{\varphi},g_{u,\omega},\mathbf{Y}^{(M)},\boldsymbol{\Theta}^{(M)})|^{lin}_{\boldsymbol{\mu}^{(M)},\boldsymbol{\beta}^{(M)},\boldsymbol{\varphi}^{(M)}}$ is the linearized Lagrangian around $\boldsymbol{\mu}^{(M)}$, $\boldsymbol{\beta}^{(M)}$ and $\boldsymbol{\varphi}^{(M)}$.The $L(\boldsymbol{\mu}^{(M)},\boldsymbol{\beta}^{(M)},\boldsymbol{\varphi}^{(M)},g_{u,\omega},\mathbf{Y}^{(M)},\boldsymbol{\Theta}^{(M)})$ is the Lagrangian of LP2 model. The LP3 model is formulated in (C.7).

$$\text{Minimize} \quad \vartheta \tag{C.7a}$$
$$\text{Subject to}$$
$$\left.\begin{array}{l} \vartheta \geq L(\boldsymbol{\mu}^B,\boldsymbol{\beta}^B,\boldsymbol{\varphi}^B,g_{u,\omega},\mathbf{Y}^{(m)},\boldsymbol{\Theta}^{(m)}|^{lin}_{\boldsymbol{\mu}^{(m)},\boldsymbol{\beta}^{(m)},\boldsymbol{\varphi}^{(m)}} \\ h^{(m)}_{k,\omega,s}(g_{u,\omega}) \leq 0, \text{ if } \boldsymbol{\mu}^B = \Xi^{\mu} \\ h^{(m)}_{k,\omega,s}(g_{u,\omega}) \geq 0, \text{ if } \boldsymbol{\mu}^B = 0 \\ \hat{h}^{(m)}_{u,\omega,s}(g_{u,\omega}) \leq 0, \text{ if } \boldsymbol{\beta}^B = \Xi^{\beta} \\ \hat{h}^{(m)}_{u,\omega,s}(g_{u,\omega}) \geq 0, \text{ if } \boldsymbol{\beta}^B = 0 \\ \tilde{h}^{(m)}_{u,\omega,s}(g_{u,\omega}) \leq 0, \text{ if } \boldsymbol{\varphi}^B = \Xi^{\varphi} \\ \tilde{h}^{(m)}_{u,\omega,s}(g_{u,\omega}) \geq 0, \text{ if } \boldsymbol{\varphi}^B = 0 \end{array}\right\} \begin{array}{l} m = 1,...,M-1, \\ m \in V \end{array} \tag{C.7b}$$

$$\left.\begin{array}{l}
\vartheta \geq L_0^{(M)}(g_{u,\omega}, \mathbf{Y}^{(M)},\ \mathbf{\Theta}^{(M)}) - \Gamma h_q^{(M)}(g_{u,\omega}) \\
h_q^{(M)}(g_{u,\omega}) \geq h_{k,\omega,s}^{(M)}(g_{u,\omega}) \\
h_q^{(M)}(g_{u,\omega}) \geq -h_{k,\omega,s}^{(M)}(g_{u,\omega}) \\
\vartheta \geq L_0^{(M)}(g_{u,\omega}, \mathbf{Y}^{(M)},\ \mathbf{\Theta}^{(M)}) - \hat{\Gamma}\hat{h}_{\hat{q}}^{(M)}(g_{u,\omega}) \\
\hat{h}_{\hat{q}}^{(M)}(g_{u,\omega}) \geq \hat{h}_{u,\omega,s}^{(M)}(g_{u,\omega}) \\
\hat{h}_{\hat{q}}^{(M)}(g_{u,\omega}) \geq -\hat{h}_{u,\omega,s}^{(M)}(g_{u,\omega}) \\
\vartheta \geq L_0^{(M)}(g_{u,\omega}, \mathbf{Y}^{(M)},\ \mathbf{\Theta}^{(M)}) - \hat{\Gamma}\tilde{h}_{\hat{q}}^{(M)}(g_{u,\omega}) \\
\tilde{h}_{\hat{q}}^{(M)}(g_{u,\omega}) \geq \tilde{h}_{u,\omega,s}^{(M)}(g_{u,\omega}) \\
\tilde{h}_{\hat{q}}^{(M)}(g_{u,\omega}) \geq -\tilde{h}_{u,\omega,s}^{(M)}(g_{u,\omega})
\end{array}\right\} \text{ If } M \in V \tag{C.7c}$$

$$\left.\begin{array}{l}
\vartheta \geq L_0^{(M)}(g_{u,\omega}, \mathbf{Y}^{(M)},\ \mathbf{\Theta}^{(M)}) + \Gamma h_q^{(M)}(g_{u,\omega}) \\
h_q^{(M)}(g_{u,\omega}) \leq h_{k,\omega,s}^{(M)}(g_{u,\omega}) \\
h_q^{(M)}(g_{u,\omega}) \leq -h_{k,\omega,s}^{(M)}(g_{u,\omega}) \\
\vartheta \geq L_0^{(M)}(g_{u,\omega}, \mathbf{Y}^{(M)},\ \mathbf{\Theta}^{(M)}) + \hat{\Gamma}\hat{h}_{\hat{q}}^{(M)}(g_{u,\omega}) \\
\hat{h}_{\hat{q}}^{(M)}(g_{u,\omega}) \leq \hat{h}_{u,\omega,s}^{(M)}(g_{u,\omega}) \\
\hat{h}_{\hat{q}}^{(M)}(g_{u,\omega}) \leq -\hat{h}_{u,\omega,s}^{(M)}(g_{u,\omega}) \\
\vartheta \geq L_0^{(M)}(g_{u,\omega}, \mathbf{Y}^{(M)},\ \mathbf{\Theta}^{(M)})\hat{\Gamma}\tilde{h}_{\hat{q}}^{(M)}(g_{u,\omega}) \\
\tilde{h}_{\hat{q}}^{(M)}(g_{u,\omega}) \leq \tilde{h}_{u,\omega,s}^{(M)}(g_{u,\omega}) \\
\tilde{h}_{\hat{q}}^{(M)}(g_{u,\omega}) \leq -\tilde{h}_{u,\omega,s}^{(M)}(g_{u,\omega})
\end{array}\right\} \text{ If } M \in V \tag{C.7d}$$

$$\text{Constraints } (11e), (11f), (11g) \tag{C.7e}$$

Where ϑ is the lower bound of the BLP problem. Term $\boldsymbol{\mu}^B$, $\boldsymbol{\beta}^B$ and $\boldsymbol{\varphi}^B$ is the upper/lower bound of $\boldsymbol{\mu}$, $\boldsymbol{\beta}$ and $\boldsymbol{\varphi}$. Indices $q \in Q$ and $\hat{q} \in \hat{Q}$ represent a subset of (k, ω, s) and (u, ω, s), respectively where $q \in \{(1,1,1), ..., (K, \Omega, S)\}$ and $\hat{q} \in \{(1,1,1), ..., (U, \Omega, S)\}$. Term $L_0^{(M)}(g_{u,\omega}, \mathbf{Y}^{(M)}, \mathbf{\Theta}^{(M)})$ represents all the terms in the linearized Lagrange function in iteration M which depends only on $g_{u,\omega}$. Scalars Γ and $\hat{\Gamma}$ is the cardinality of sets Q and $\hat{Q}$. Inequalities (C.7b) represent the linearized Lagrange functions from the previous $M-1$ iterations. Floudas (2000) shows that the minimum value of ϑ is achieved at the minimum or maximum value of $h_q^{(M)}(g_{u,\omega})$, $\hat{h}_{\hat{q}}^{(M)}(g_{u,\omega})$ and $\tilde{h}_{\hat{q}}^{(M)}(g_{u,\omega})$. Inequalities (C.7c) assume $h_q^{(M)}(g_{u,\omega})$, $\hat{h}_{\hat{q}}^{(M)}(g_{u,\omega})$ and $\tilde{h}_{\hat{q}}^{(M)}(g_{u,\omega})$ are at its maximum value and inequalities (C.7d) assume $h_q^{(M)}(g_{u,\omega})$, $\hat{h}_{\hat{q}}^{(M)}(g_{u,\omega})$ and $\tilde{h}_{\hat{q}}^{(M)}(g_{u,\omega})$ are at its minimum value. Two subproblems (one assumes $h_q^{(M)}(g_{u,\omega})$, $\hat{h}_{\hat{q}}^{(M)}(g_{u,\omega})$ and $\tilde{h}_{\hat{q}}^{(M)}(g_{u,\omega})$ are at their maximum value and the other one as-

sumes $h_q^{(M)}(g_{u,\omega})$, $\hat{h}_{\hat{q}}^{(M)}(g_{u,\omega})$ and $\tilde{h}_{\hat{q}}^{(M)}(g_{u,\omega})$ are at their minimum value) are formulated. Subproblem 1 is formulated by (C.7a), (C.7b), (C.7c) and (C.7e). Similarly, subproblem 2 is formulated by (C.7a), (C.7b), (C.7d) and (C.7e). These two subproblems are solved for each u, k, ω, s and the minimum value of ϑ is the lower bound of the BLP problem. If the LP2 model in iteration M is infeasible, the Lagrangian from the feasibility model LP2 is formed and used in the LP3 model, see Floudas (2000).

The steps of the combined NGBD-PRD solution algorithm is detailed in Steps (0)-(12)

Step 0 Set UB_1 and UB_2 to $+\infty$ and LB_1 to $-\infty$. Set tolerance ε. Set given integer decisions. Go to Step 1.

Step 1 Go to Step 2, if $(LB_1 < UB_1)$ and $(LB_1 < UB_2 - \varepsilon)$. Otherwise go to Step 7.

Step 2 Set y=y+1. Solve the LP1-R model and calculate $\hat{\epsilon}_{\omega,s}$. Set $\bar{\epsilon}_{\omega,s}$=$\hat{\epsilon}_{\omega,s}$ in the LP1. Solve the LP1 model. Go to Step 3, if it is feasible. Otherwise go to Step 4.

Step 3 Add an optimality cut to problem (C.5). Add set $E^{(y)} = E^{(y-1)} \cup \{y\}$. Update $UB_1 = min(UB_1, \Upsilon)$. Go to Step 5.

Step 4 Solve the feasibility LP1 model. Add a feasibility cut to problem (C.5). Add set $O^{(y)} = O^{(y-1)} \cup \{y\}$. Go to Step 5.

Step 5 Solve the RMILP problem in (C.5). Set $LB_1 = \varrho$ and store the solution of (C.5) in $\bar{\boldsymbol{b}}^{(y+1)}$=$\bar{\boldsymbol{b}}^{*}$. Go to Step 6.

Step 6 Go to Step 7, if $LB_1 \geq UB_1$. Otherwise go to Step 2.

Step 7 Terminate if $UB_1 \geq UB_2$. Otherwise go to Step 8.

Step 8 Fix $\boldsymbol{b}$=$\bar{\boldsymbol{b}}^{(y)}$ and Solve the BLP problem using steps (8-a)-(8-g).

Step 8-a Set UB_2 to $+\infty$ and LB_2 to $-\infty$. Set $g_{u,\omega}^{(M)} = g_{u,\omega}^{(e)}$. Go to Step 8-b.

Step 8-b Solve the LP2-R model and store $\hat{\epsilon}_{\omega,s}$. Go to Step 8-c.

Step 8-c Fix $\bar{\epsilon}_{\omega,s} = \hat{\epsilon}_{\omega,s}$ in LP2 and solve the LP2 model for $g_{u,\omega} = \bar{g}_{u,\omega}^{(M)}$. If it is feasible, add M to V. Update $UB_2 = min(UB_2, \Psi)$. If the LP2 model is infeasible, add M to Z and solve the feasibility LP2 model. Go to Step 8-d.

Step 8-d Evaluate $h^{m}_{k,\omega,s}(g_{u,\omega})$ for all previous $M-1$ iterations and select one Lagrange function for each previous iteration using the procedure below and go to Step 8-e.

- If $h^{(m)}_{k,\omega,s}(g^{(M)}_{u,\omega}) \geq \varepsilon$, set $\boldsymbol{\mu}^B = 0$
- If $h^{(m)}_{k,\omega,s}(g^{(M)}_{u,\omega}) \leq -\varepsilon$, set $\boldsymbol{\mu}^B = \Xi^{\mu}$
- If $\hat{h}^{(m)}_{u,\omega,s}(g^{(M)}_{u,\omega}) \geq \varepsilon$, set $\boldsymbol{\beta}^B = 0$
- If $\hat{h}^{(m)}_{u,\omega,s}(g^{(M)}_{u,\omega}) \leq -\varepsilon$, set $\boldsymbol{\beta}^B = \Xi^{\beta}$
- If $\tilde{h}^{(m)}_{u,\omega,s}(g^{(M)}_{u,\omega}) \geq \varepsilon$, set $\boldsymbol{\varphi}^B = 0$
- If $\tilde{h}^{(m)}_{u,\omega,s}(g^{(M)}_{u,\omega}) \leq -\varepsilon$, set $\boldsymbol{\varphi}^B = \Xi^{\varphi}$

Step 8-e Solve subproblem 1 and subproblem 2 for $\forall q \in Q$ and $\forall \hat{q} \in \hat{Q}$. If it is feasible, store ϑ and $g_{u,\omega}$. Go to Step 8-f.

Step 8-f Select the minimum value of the stored ϑ and the corresponding $g_{u,\omega}$. Update the lower bound $LB_2 = \vartheta^{min}$ and set $g^{(M+1)}_{u,\omega} = g^{min}_{u,\omega}$. Go to Step 8-g

Step 8-g Go to Step 9 if $UB_2 - LB_2 < \varepsilon$. Otherwise go to Step 8-a.

Step 9 Set $R^f = R^{f-1} \cup \{y\}$. Update $UB_2 = min(UB_2, \Psi)$. Go to Step 10.

Step 10 Go to Step 11, if $E \setminus R \neq \emptyset$. Otherwise set $UB_1 = \infty$ and go to Step 12.

Step 11 Pick $v \in E^{(y)} \setminus R^{(f)}$ such that $\Upsilon^{(v)} = min_{w \in E^y \setminus R^f} \Upsilon^w$. Update $UB_1 = \Upsilon^v$. Set $\bar{\boldsymbol{b}}^{(y)} = \bar{\boldsymbol{b}}^{(v)}$ and $y = v$. Go to Step 12.

Step 12 Terminate if $UB_1 \geq UB_2$ and $LB_1 \geq UB_2 - \varepsilon$. Otherwise, go to Step 1.

The solution algorithm is coded by the authors in GAMS' platform. LP1, LP1-R, RMILP, LP2 and LP2-R models are solved by the CPLEX solver, the LP3 model is solved by the MOSEK solver. The codes are run on a computer with two CPUs each with 2.30 GHz clocking frequency and 128 GB of RAM.

Appendix D. The details of replacement of complementary slackness conditions by strong duality conditions

The complementary slackness conditions of (1d-1i) are written in D.1.

$$\mu_{k,\omega,s}\big(F_k - \sum_n H_{k,n}(\sum_{n:u}(g_{u,\omega} + g^{up}_{u,\omega,s} - g^{dn}_{u,\omega,s}) - v_{n,\omega,s} - D_{n,\omega} + \Delta W_{n,\omega,s})\big) = 0,\ \forall k,\omega,s \quad \text{(D.1a)}$$

$$\kappa_{u,\omega,s} g^{up}_{u,\omega,s} = 0,\ \forall u,\omega,s \quad \text{(D.1b)}$$

$$\beta_{u,\omega,s}(G_u - g_{u,\omega} - g^{up}_{u,\omega,s}) = 0,\ \forall u,\omega,s \quad \text{(D.1c)}$$

$$\psi_{u,\omega,s} g^{dn}_{u,\omega,s} = 0,\ \forall u,\omega,s \quad \text{(D.1d)}$$

$$\varphi_{u,\omega,s}(g_{u,\omega} - g^{dn}_{u,\omega,s}) = 0,\ \forall u,\omega,s \quad \text{(D.1e)}$$

$$\theta_{n,\omega,s} v_{n,\omega,s} = 0,\ \forall n,\omega,s \quad \text{(D.1f)}$$

$$\chi_{n,\omega,s}(\bar{W}_{n,\omega} + \Delta W_{n,\omega,s} - v_{n,\omega,s}) = 0,\ \forall n,\omega,s \quad \text{(D.1g)}$$

We can prove that the strong duality condition in (2e) is the exact reformulation of the complementary slackness conditions in (D.1) using the following the steps below:

Step 1 Multiply both sides of stationary conditions (2a), (2b) and (2c) by $g^{up}_{u,\omega,s}$, $g^{dn}_{u,\omega,s}$ and $v_{n,\omega,s}$, respectively. Sum the left-hand sides and obtain an equality which has a right-hand side value zero.

Step 2 Sum the both sides of all equalities in (D.1) and obtain an equality which has a right-hand side value zero.

Step 3 Subtract left-hand side of the equality obtained in Step 1 from the equality obtained in Step 2.

Step 4 From (1e), replace $\sum_{n:u}(g^{up}_{u,\omega,s} - g^{dn}_{u,\omega,s}) - v_{n,\omega,s}$ by $D_{n,\omega} - \Delta W_{n,\omega,s} - \sum_{n:u} g_{u,\omega}$. The resulting equality is exactly the same with (2e).

Given the day-ahead decisions, Table D.15 shows the nonlinear terms and the number of constraints in two cases: (a) The KKT condition with complementary slackness conditions and (b) the KKT conditions with strong duality condition.

It can be seen from Table D.15 that replacing the complementary slackness conditions by the strong duality conditions reduces the total number of constraints from $(K + 4U + 2N)\text{x}\Omega\text{x}S$ to $\Omega\text{x}S$. Moreover the number of nonlinear terms reduces from $(3K + 4U + 2N)\text{x}\Omega\text{x}S$ to zero.

Table D.15: The nonlinear terms and the number of constraints in Case (a) (KKT conditions with complementary slackness conditions) and in Case (b) (KKT conditions with strong duality condition), K: Number of transmission lines, U: Number of producers, N: Number of nodes, Ω, S: Number of imbalance scenarios.

	Constraints	Nonlinear terms	#constraints	#nonlinear terms
Case (a)	(D.1a)	$\mu_{k,\omega,s} \sum_n H_{k,n} (\sum_{n:u} g^{up}_{u,\omega,s})$ $\mu_{k,\omega,s} \sum_n H_{k,n} (\sum_{n:u} g^{dn}_{u,\omega,s})$ $\mu_{k,\omega,s} \sum_n H_{k,n} v_{n,\omega,s}$	KxΩxS	3xKxΩxS
	(D.1b)	$\kappa_{u,\omega,s} g^{up}_{u,\omega,s}$	UxΩxS	UxΩxS
	(D.1c)	$\beta_{u,\omega,s} g^{up}_{u,\omega,s}$	UxΩxS	UxΩxS
	(D.1d)	$\psi_{u,\omega,s} g^{dn}_{u,\omega,s}$	UxΩxS	UxΩxS
	(D.1e)	$\varphi_{u,\omega,s} g^{dn}_{u,\omega,s}$	UxΩxS	UxΩxS
	(D.1f)	$\theta_{n,\omega,s} v_{n,\omega,s}$	NxΩxS	NxΩxS
	(D.1f)	$\chi_{n,\omega,s} v_{n,\omega,s}$	NxΩxS	NxΩxS
Case (b)	(2e)	-	ΩxS	0

References

Alaywan, Z., Wu, T., Papalexopoulos, A. D., Oct 2004. Transitioning the california market from a zonal to a nodal framework: an operational perspective. In: IEEE PES Power Systems Conference and Exposition, 2004. Vol. 2. pp. 862–867.

Bjørndal, E., Bjørndal, M., Gribkovskaia, V., 2012. Congestion management in the nordic power market: nodal pricing versus zonal pricing. Tech. Rep. 15, SNF, NHH.

Bjørndal, M., Jörnsten, K., 2007. Benefits from coordinating congestion managementthe nordic power market. Energy Policy 35 (3), 1978 – 1991.

Bjørndal, M., Jörnsten, K., Pignon, V., 2003. Congestion management in the nordic power market counter purchases and zonal pricing. Journal of Network Industries os-4 (3), 271–292.
URL `https://doi.org/10.1177/178359170300400302`

Boyd, S., Vandenberghe, L., 2004. Convex Optimization. Cambridge University Press, New York, NY, USA.

Chao, H.-P., Peck, S., Sep 1998. Reliability management in competitive electricity markets. Journal of Regulatory Economics 14 (2), 189–200.

Costa, A., Liberti, L., 2012. Relaxations of multilinear convex envelopes: Dual is better than primal. In: Klasing, R. (Ed.), Experimental Algorithms. Springer Berlin Heidelberg, Berlin, Heidelberg, pp. 87–98.

Dijk, J., Willems, B., Mar. 2011. The Effect of Counter-trading on Competition in Electricity Markets. Energy Policy 39 (3), 1764–1773.

Floudas, C. A., 2000. The gop primal–relaxed dual decomposition approach: theory. In: Deterministic Global Optimization: Theory, Methods and Applications. Vol. 37. Springer US, Boston, MA, pp. 67–139.

Fuller, J. D., Celebi, E., 2017. Alternative models for markets with nonconvexities. European Journal of Operational Research 261 (2), 436 – 449.

Gabriel, S., Conejo, A., Fuller, J., Hobbs, B., Ruiz, C., 2012. Complementarity Modeling in Energy Markets. International Series in Operations Research & Management Science. Springer New York.

Gabriel, S. A., Sep 2017. Solving discretely constrained mixed complementarity problems using a median function. Optimization and Engineering 18 (3), 631–658.
URL https://doi.org/10.1007/s11081-016-9341-2

Gabriel, S. A., Conejo, A. J., Ruiz, C., Siddiqui, S., 2013a. Solving discretely constrained, mixed linear complementarity problems with applications in energy. Computers and Operations Research 40 (5), 1339 – 1350.

Gabriel, S. A., Siddiqui, S. A., Conejo, A. J., Ruiz, C., Sep 2013b. Solving discretely-constrained nash–cournot games with an application to power markets. Networks and Spatial Economics 13 (3), 307–326.
URL https://doi.org/10.1007/s11067-012-9182-2

Green, R., 2007. Nodal pricing of electricity: how much does it cost to get it wrong? Journal of Regulatory Economics 31 (2), 125–149.

Grigg, C., Wong, P., Albrecht, P., Allan, R., Bhavaraju, M., Billinton, R., Chen, Q., Fong, C., Haddad, S., Kuruganty, S., Li, W., Mukerji, R., Patton, D., Rau, N., Reppen, D., Schneider, A., Shahidehpour, M., Singh, C.,

Aug 1999. The ieee reliability test system-1996. a report prepared by the reliability test system task force of the application of probability methods subcommittee. IEEE Transactions on Power Systems 14 (3), 1010–1020.

Gupta, A., Jain, R., Poolla, K., Varaiya, P., Dec 2015. Equilibria in two-stage electricity markets. In: Proc. 2015 54th IEEE Conference on Decision and Control (CDC). pp. 5833–5838.

Gupte, A., Ahmed, S., Cheon, M. S., Dey, S., 2013. Solving mixed integer bilinear problems using milp formulations. SIAM Journal on Optimization 23 (2), 721–744.

Harvey, S. M., Hogan, W. W., 2000a. Nodal and Zonal Congestion Management and the Exercise of Market Power. Harvard University, http://ksghome. harvard. edu/˜. whogan. cbg. ksg.

Harvey, S. M., Hogan, W. W., 2000b. Nodal and Zonal Congestion Management and the Exercise of Market Power: Further Comments. Harvard University, http://ksghome. harvard. edu/˜. whogan. cbg. ksg 11.

Hesamzadeh, M. R., Biggar, D. R., Aug 2012. Computation of extremal-nash equilibria in a wholesale power market using a single-stage MILP. Power Systems, IEEE Transactions on 27 (3), 1706–1707.

Hesamzadeh, M. R., Biggar, D. R., May 2013. Merger analysis in wholesale power markets using the equilibria-band methodology. IEEE Transactions on Power Systems 28 (2), 819–827.

Holmberg, P., Lazarczyk, E., 2015. Congestion Management in Electricity Networks: Nodal, Zonal and Discriminatory Pricing. Energy Journal 36 (2), 145 – 166.

Hu, X., Ralph, D., Oct 2007. Using epecs to model bilevel games in restructured electricity markets with locational prices. Operations research 55 (5), 809–827.

Huppmann, D., Siddiqui, S., 2018. An exact solution method for binary equilibrium problems with compensation and the power market uplift problem. European Journal of Operational Research 266 (2), 622 – 638.

Li, X., Tomasgard, A., Barton, P. I., Dec 2011. Nonconvex generalized benders decomposition for stochastic separable mixed-integer nonlinear programs. Journal of Optimization Theory and Applications 151 (3), 425.

McCormick, G. P., 1976. Computability of global solutions to factorable nonconvex programs: Part i — convex underestimating problems. Mathematical Programming 10 (1), 147–175.

Neuhoff, K., Hobbs, B., Newbery, D. M., 2011. Congestion management in european power networks: Criteria to assess the available options. Discussion Papers of DIW Berlin 1161, DIW Berlin, German Institute for Economic Research.
URL https://EconPapers.repec.org/RePEc:diw:diwwpp:dp1161

Ruderer, D., Zöttl, G., 2012. The impact of transmission pricing in network industries. Cambridge Working Papers in Economics 1230, Faculty of Economics, University of Cambridge.
URL https://ideas.repec.org/p/cam/camdae/1230.html

Ruiz, C., Conejo, A. J., Gabriel, S. A., Aug 2012. Pricing non-convexities in an electricity pool. IEEE Transactions on Power Systems 27 (3), 1334–1342.

Stoft, S., 1999. Financial transmission rights meet cournot: How tccs curb market power. The Energy Journal 20 (1), 1–23.

Tawarmalani, M., Sahinidis, N. V., June 2005. A polyhedral branch-and-cut approach to global optimization. Mathematical Programming 103 (2), 225–249.

Van den Bergh, K., Boury, J., Delarue, E., 2016. The flow-based market coupling in central western europe: Concepts and definitions. The Electricity Journal 29 (1), 24 – 29.

Willems, B., 2002. Modeling cournot competition in an electricity market with transmission constraints. The Energy Journal 23 (3), 95–125.

Zhang, D., Kim, S., June 2010. A two stage stochastic equilibrium model for electricity markets with forward contracts. In: Proc. 2010 11th International Conference on Probabilistic Methods Applied to Power Systems (PMAPS). pp. 194–199.

Zhang, D., Xu, H., Dec 2013. Two-stage stochastic equilibrium problems with equilibrium constraints: modeling and numerical schemes. Optimization 62 (12), 1627–1650.

Zhang, D., Xu, H., Wu, Y., Feb 2010. A two stage stochastic equilibrium model for electricity markets with two way contracts. Mathematical Methods of Operations Research 71 (1), 1–45.